A COMPARISON OF RECLASSIFICATION METHODS TO IMPROVE AN NDVI BASED FLOOD MAP

by

Jessica V. Fayne

A Thesis
Submitted to the
Graduate Faculty
of
George Mason University
in Partial Fulfillment of
The Requirements for the Degree
of
Master of Science
Geographic and Cartographic Sciences

Committee:

_____	Dr. Sven Fuhrmann, Thesis Director
_____	Dr. Matthew T. Rice, Committee Member
_____	Dr. Paul R. Houser, Committee Member
_____	Dr. John D. Bolten, Committee Member
_____	Dr. Anthony Stefanidis, Department Chair
_____	Dr. Donna M. Fox, Associate Dean, Office of Student Affairs & Special Programs, College of Science
_____	Dr. Peggy Agouris, Dean, College of Science

Date: _____ Spring Semester 2015
George Mason University
Fairfax, VA

A Comparison of Reclassification Methods to Improve an NDVI Based Flood Map

A Thesis submitted in partial fulfillment of the requirements for the degree of
Master of Science at George Mason University

by

Jessica V. Fayne
Bachelor of Arts
Hampton University, 2010

Director: Sven Fuhrmann, Associate Professor
Department of Geographic and Geoinformation Sciences

Spring Semester 2015
George Mason University
Fairfax, VA

DEDICATION

This is dedicated to my family, supporters, and anyone who will benefit from this research. Thank you for your time and attention.

ACKNOWLEDGEMENTS

I would like to thank the many family members, friends, and supporters who have allowed me to make this happen.

I also wish to thank my advisors at George Mason and NASA GSFC and the George Mason University GGS staff members who supported my research and continued exploration into remote sensing.

My previous remote sensing professors gave me the background knowledge to pursue my interests.

My experience in the NASA DEVELOP program provided me the opportunity to increase my knowledge of remote sensing, GIS, and programming, DEVELOP team members from Mekong Flood Disasters and Himalayan Flood Disasters were essential in my learning of the R statistical programming language, to make data processing at this scale possible.

TABLE OF CONTENTS

LIST OF TABLES

LIST OF FIGURES

LIST OF ABBREVIATIONS

Moderate Resolution Imaging Spectroradiometer ..... MODIS
Advanced Very High Resolution Radiometer ..... AVHRR
Normalized Difference Vegetation Index ..... NDVI
Normalized Difference Water Index ..... NDWI
Geographic Information System ..... GIS

ABSTRACT

A COMPARISON OF RECLASSIFICATION METHODS TO IMPROVE AN NDVI BASED FLOOD MAP

Jessica V. Fayne, MS

George Mason University, 2015

Thesis Director: Dr. Sven Fuhrmann

In Cambodia and Vietnam, low-lying terrain is particularly susceptible to flooding during the monsoon season between May and November. To monitor flooding in the region, a near-real time NDVI percent decrease based Flood Extent Product was developed to be hosted on an online Flood Dashboard by the NASA DEVELOP team. The product was designed to be updated twice per day with 250-meter resolution from MODIS on the Aqua and Terra satellites. To increase the usage and usability of this product, the classification intervals were compared with other commonly used classification schemes to monitor flooding.

The use of substantiated flood classification methods is essential to ensure understanding and usefulness of mapped flood products. Classification schemes can influence the usability and usefulness of these products, e.g. inappropriate flood mapping classification intervals and color selections may incorrectly classify flooded areas and distract from the interpretation of the phenomenon of interest.

The percent change method proved to be very helpful in delineating flood boundaries compared to standard deviation and differencing methods. However, only the 100% decrease interval class had the highest accuracy ratings compared to three reference data sets, with an average producer's accuracy of 67.8% and an average user's accuracy of 74%. The results of the accuracy assessments indicate that only the 100% interval class can be reclassified to into a descriptive 'flood' classification. The use of an additional 'wet' category with 75% decrease will be useful to support the flooded area description and allow users to monitor changes in regions that are not currently flooded, but are more susceptible to flooding. The use of a descriptive two-class product eliminates confusion from understanding input data while removing extra information from lower interval change classes.

RESEARCH PROBLEM

Introduction

As part of the Committee on Earth Observing Satellites (CEOS) Working Group on Disasters Flood Pilot Program, the NASA DEVELOP Disasters team at Goddard Space Flight Center created a satellite-based flood extent product for the Lower Mekong River Basin (LMB) in Southeast Asia. The goals of the CEOS Working Group on Disasters Flood Pilot are to demonstrate that value of earth observing satellites by integrating data from flood modeling and monitoring systems and at global and regional scales (CEOS WGDisasters 2015). Running through China, Laos, Thailand, Cambodia and Vietnam, the flooding of the Mekong River is an issue of international importance, with potential to earn the area millions of dollars in crop revenue, or cost millions more in from possible loss of life and damage to villages. The costs can be mitigated by governing and planning organizations by such as the Mekong River Commission (MRC), and local leadership for disaster planning and the ability to locate defined areas affected by flooding.

The NASA DEVELOP team created the Flood Extent Product by using NDVI calculated from red and infrared surface reflectance from the Moderate Resolution Imaging Spectroradiometer (MODIS) sensor from the Terra and Aqua satellites, which have a sun-synchronous orbit. The use of the two satellites allows two observations per day for a higher temporal resolution while avoiding cloud effects. MODIS scans the

earth using visible reflectance (short) and thermal emittance (long) wavelengths. The data generated for the Flood Product was created using visible Red and Infrared wavelengths at a 250-meter spatial resolution as inputs to the Normalized Difference Vegetation Index (NDVI). The Normalized Difference Vegetation Index is a spectral index that commonly used to calculate the health of vegetation; in this instance, NDVI is used to monitor decrease in vegetation during the flood season to infer additional water presence. The NDVI anomaly method was suggested to the develop team by DEVELOP advisor Joseph Spruce, who used a similar method for deforestation caused by gypsy moth infestation (Spruce, et al. 2011), additional authors similarly use vegetation and other related spectral indices to determine flooding (Boshetti, et al. 2014). The Flood Extent Product categorizes the percent NDVI decrease into seven classes (0%, 4%, 15%, 30%, 50%, 75%, and 100%), ranging in color from blue to red (0% is no or positive change-transparent, 4% is blue, and 100% is red).

The seven class structure is somewhat biased in the assumption that all NDVI decreases correspond with increased water presence. The first six classes correspond directly with the actual values derived from the calculation, but the 100% decrease value encompasses decreases of 100% and more. This truncation may be confusing as the baseline NDVI values are not referenced in the final product, and therefore the amount of change over 100% will have varying implications based on the original pixel value.

Positive NDVI values generally correspond to the health of vegetation; however, negative NDVI values may be caused by a variety of factors such as a complete lack of vegetation, burned areas, snow, water, minerals, sediment, and many other non-

vegetation land covers. Because of the diversity of land cover represented by negative NDVI or by decreases in NDVI, it is problematic to infer that the area is flooded due to the decrease in NDVI values. The NDVI anomaly method is particularly challenging during the dry season, when decreased values are often associated with drought and drying vegetation.

Research Questions

This study asks a few questions to form a more comprehensive understanding of the baseline NDVI values:

- How does the land cover help distinguish between NDVI change caused by flooding or other factors?
    - How could NDVI values be classified into meaningful qualitative categories to improve interpretation?
- Would existing literature on the visualization of flood mapping products help to explain how the Flood Extent Product would be used and understood?
    - What are the design requirements for a flood-mapping product? How does literature on flood mapping provide guidelines for color use and classification?
- Can understanding the baseline NDVI values and associated NDVI change values explain how the product works and the implications of the NDVI change values?
    - How will understanding the NDVI change values make the product usable with additional datasets and maps?

Scope of Work

A known limitation of the Flood Extent Product stems from the lack of knowledge about the baseline NDVI. The percent decrease at each pixel will be a function of the original NDVI number—smaller numbers will exhibit a larger decrease, such as an original NDVI of 0.04→-0.2 will yield a 400% decrease, although an NDVI of -0.2 would not necessarily mean there is water on the ground. In contrast, a 4% decrease in NDVI is difficult to attribute to water presence. This uncertainty in the product is not

currently addressed; however, researchers have developed several methods to associate uncertainty information with the visualized product.

The role of spectral indices is very significant to this research, as the meaning and the assumptions made by the indices have the capacity to bias any product that employs indices without an assessment of the implications of limitations of the index calculation. A review of spectral indices created specifically for flood mapping as well as non-traditional indices that can be incorporated into flood maps will help to direct the research on the effects of the NDVI percent decrease method.

A review of other flood mapping products used by organizations in South East Asia, as well as other flood products may support or reject the visualization and format of the Flood Extent Product. As the product was created with the intention to be passed along to the Mekong River Commission, it is important that the product conform to the standards of the target audiences, as well as cartographic convention for flood mapping.

LITERATURE REVIEW

The classification of spectral indices, particularly NDVI anomaly is at the core of this research, as understanding what negative NDVI means for flooding is important to the classification of flooded areas. Related spectral indices targeted towards flood and water delineation techniques guide the use of NDVI as a flood product where areas that exhibit NDVI decrease, but not flooding, can be considered in the product. Finally, a review of the use of color schemes and mapping products—online and static are considered for the purpose of visually associating higher decreases in NDVI with more water.

NDVI Anomaly

A known limitation of the Flood Extent Product stems from the lack of knowledge about the baseline NDVI. The percent decrease at each pixel will be a function of the original NDVI number—smaller numbers will exhibit a larger decrease, such as an original NDVI of 0.04→ -0.2 will yield a 400% decrease, although an NDVI of -0.2 would not necessarily mean there is water on the ground. Similarly, a small 4% decrease in NDVI is difficult to attribute to water presence.

The Normalized Difference Vegetation Index (NDVI) and other vegetation spectral indices were created with the purpose of monitoring the health of vegetation and crop yields (Rouse Jr., et al. 1973, Tucker 1979, Colwell 1974). The creation of these vegetation spectral indices gave rise to new developments in phenology, drought monitoring and the creation of land cover products. Vegetation indices use the visible red

and near infrared wavelengths to determine the health of vegetation as a function of the brightness of photo synthetically active vegetation to the background soil observation (Colwell 1974). Many authors have used vegetation indices to monitor vegetation and changes in the environment over time, as the index outputs only give a static view of the current state of the physical environment. To understand change over time, basic image subtraction (Sarp 2011) and percent change methods (Murad and Saiful Islam 2011) can be used to see how much an area has changed. In addition to changes between a few images, several projects looked at many images over several decades for a long-term trend analysis of the physical environment to aid with modeling and climate analysis (Nash, et al. 2014, Jönsson, et al. 2010). Others (Gopinath, et al. 2014) created a web-based monitoring system to monitor decrease in NDVI as a measure of drought.

In (Nash, et al. 2014), researchers studied the change in greenness over New Mexico, USA, with 1-km NDVI pixels derived from the AVHRR (Advanced Very High Resolution Radiometer) satellite from 1989-2006. The study utilized a univariate and multivariate method (without and with climate as an additional variable) to the relationship of NDVI over time. The AVHRR sensor series was the predecessor to the MODIS sensor with the first AVHRR launched in 1978 with subsequent modifications and launches in 1989 and 1998 (NOAA SIS 2013), which allows researchers to conduct times series studies using a longer data record. Using NDVI from AVHRR helped to create a baseline of seasonal variation that is evident in NDVI scenes throughout the year to understand the actual increase or decrease in NDVI for that date. Nash et al. identifies

four local features that contribute to the change in NDVI outside the realm of variation in climate:

- Agricultural changes from farming and irrigation at select times of the year for select crops
- Prolonged fires in selected pixels showed decreases in NDVI as well as a steady decrease in the post-fire period as the mortality increased for effected vegetation
- The manifestation of invasive vegetation species over a recently burned area contributed to a rapid increase in NDVI
    - Human use of the region around the Rio Grande contributed to the reduction of water and lowering the water table in the area, compounding the impact of droughts
- Several forested areas in the study region were vulnerable to defoliation caused by the bark beetle insect infestation

In contrast to a longitudinal study of NDVI over time, authors used higher temporal resolution images from TERRA MODIS and AVHRR to develop drought-monitoring maps over the study area (Gopinath, et al. 2014, Murad and Saiful Islam, Drough Assessment using remote sensing and GIS in North-West region of Bangladesh 2011, Song, et al. 2004). Gopinath et al. used the 16-day Terra MODIS 250 meter NDVI composite to create a 13 year mean from which to derive a daily anomaly for drought risk areas. The negative anomaly indicates 'below normal vegetation condition' which is an

indicator of drought, however, it is important to note that low NDVI does not always correspond to drought. The NDVI anomaly was classified based on a qualitative scheme by (Murad and Saiful Islam 2011). The addition of a Land Use/Land Cover map aided localized assessment of drought risk by crop type.

The anomaly NDVI is calculated by the equation presented in (Murad and Saiful Islam 2011):

$$Anomaly\ NDVI\ i = \frac{NDVI \max i - mean\ NDVI\ max}{mean\ NDVI\ max} * 100$$

This will yield values on a ±100% scale, when 0 to -10% is slight drought, -10 to -20% is moderately drought, -20 to -30% is severe drought, and above 30% is considered very severe drought (Murad and Saiful Islam, Drough Assessment using remote sensing and GIS in North-West region of Bangladesh 2011). While the percent anomaly values were given qualitative classification, there is no explanation for how these classes were created or accuracy assessment based on the classification scheme. Fortunately, Murad and Islam's project also included the use of meteorological data in the form of the Standardized Precipitation Index over the study area, where the SPI drought forecast was combined with the NDVI based drought classification for a final drought risk map; the domain specific classification was balanced by meteorological assessment.

The combination of supporting datasets is a commonly used practice in remote sensing to develop a more comprehensive product with higher accuracy and information. Researchers in (Gopinath, et al. 2014) modeled their drought risk product after (Abbas, et al. 2014) where the Normalized Vegetation Supply Water Index (NVSWI) was developed by normalizing the VSWI—given by the ratio of NDVI/Land Surface Temperature,

giving meaning and comparable values to the region and over the longitudinal study period. The subsequent value ranges specific to the years observed, 0-100 present a scale where zero is the driest pixel during the study period and 100 is the wettest. The NVSWI was then combined with land use/land cover maps and climate data to determine relative drought risk over time.

Another method to determine NDVI change in the region was used over East Asia in (Song, et al. 2004) by differencing the up-to-date NDVI with the standard image, which yielded local pixel values in line with the NDVI scale. The associated legend displays values below -0.25 in red (where drought risk is implied, but not explicitly stated), -0.1 to -0.25 in yellow, 0.1 to -0.1 in grey (within normal range), 0.1 to 0.25 in light blue, while pixels over 0.25 are green. While there is limited qualitative nomenclature in the mapped product, the assumptions for the user are reduced by keeping values in the original units of measurement using evenly spaced classes on either side of zero.

In contrast to using the percent change method, the NDVI amount of decline used in (Song, et al. 2004), has clearer implications for varying rates of change throughout the image. Specifically, because NDVI's values range between -1 and 1, the amount of decrease can only be 2 at the most extreme case using NDVI values, however percent change values can exceed 200% change, which can be difficult to interpret into meaningful information, as classified in (Murad and Saiful Islam 2011). A possible answer to this problem is seen in (Abbas, et al. 2014), when the NVSWI was classified into 5 equal interval classes (on a scale of 0-100: severe drought <20, moderate drought

20-40, slight drought 40-60, normal 60-80, and wet >80), assuming a normal distribution of values which supports the indication of extreme dry and wet conditions. Similarly, (Cai, Du and Liu 2010) implement a density slice classification for extreme, severe, moderate, and slight drought, and normal dryness.

Spatial Resolution refers to how clear and sharp the sensor can view the land. Imaging spatial resolution is measured in pixel sizes—the size of the image cells that make up the image, and the amount of land those cells represent. For example, '1-kilometer resolution' means that the pixels in the image average everything in one square kilometer segments. Generally, the satellite spatial resolution is related to the temporal resolution: sensors that physically closer to Earth may have a higher spatial resolution because it can view the object more clearly. However, because the sensor is close Earth, or the swath of the image is small, the amount of time it takes to orbit the entire earth and come back to the same location will be much longer than another satellite, which is viewing from farther away, but has a lower spatial resolution and large swath.

Some drawbacks to the use of NDVI relate to data processing and collection errors, as well as errors caused by spatial resolution and registration (Pettorelli, et al. 2009). NDVI is subject to noise errors caused by a multitude of factors such as cloud cover, scan angle, snow, shadows, or water (Pettorelli, et al. 2009). These errors can create false high or low NDVI values, which are disruptive to analysis tracking positive or negative trends in NDVI. While many studies mentioned here used pixel based analysis to monitor NDVI change values, (Pettorelli, et al. 2009) lists several factors that

can contribute to pixel variation over time, these effects may not be critical in certain spatial resolution studies:

- Plant Architectural Arrangement
- Interactions With Canopy Cover
- Height
- Composition Of Species
- Vegetation Vigor
- Leaf Properties
- Vegetation Stress
- Topography
- Altitude

In addition to the possible errors listed above, the most common error comes from the presence of cloud cover (Anderson, et al. 2007, Pettorelli, et al. 2009, Holben 2007), which obscures the surface reflectance and causes irregularities with masking and compositing images. Smoothing techniques such as the Best Index Slope Extraction (BISE), maximum-value and curve fitting from (Holben 2007, van Dijk, et al. 1987), and regression based techniques (Zhang, et al. 2003, Swets, et al. 1999) present methods to isolate anomalies based on predicted values.

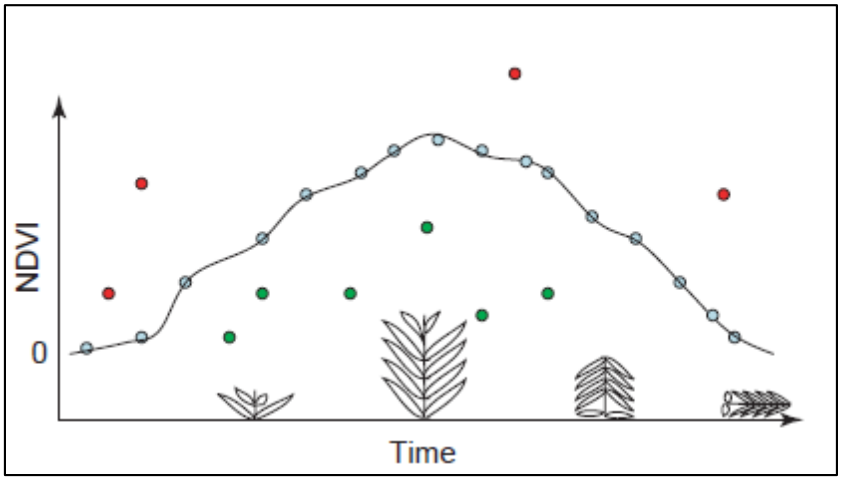

Figure 1. NDVI time series smoothing explanation: cloudy NDVI pixels are shown in green, clear day observations are shown in blue, and transmission errors are shown in red. The black line presents smoothing over the clear day observations. (Pettorelli, et al. 2009)

In (van Dijk, et al. 1987), researchers note that the swath size and therefore the incident angle over the terrain relative nadir is an important feature to note where larger swaths sizes evident in AVHRR have a larger scan angle of 56°, compared to the 7.5° angle of Landsat TM.

Flood Mapping from Space

The meaning and the assumptions made by the indices have the capacity to bias any product that employs indices without an assessment of the implications of limitations of the index calculation. A review of spectral indices created specifically for flood mapping as well as non-traditional indices and interpretation methods that can be incorporated into flood maps will help to direct the research on the effects of the NDVI percent decrease method.

Visual interpretation is a commonly used and simple method for classification of visual ground features. It is important to note that while it is generally agreed that data

from the Landsat series has a more ideal spatial resolution than most earth observing satellites, Landsat's observation rate is every 16 days, compared to daily images from more coarse resolution sensors such as MODIS and AVHRR. The Landsat name refers to a collection of satellites that have a data record going back to 1972, with spatial resolution from visible bands varying between 60-15 meters over seven generations (USGS 2015). One example of the use of daily observations is seen in (Rasid and Pramanik 1990) where flooding in Bangladesh was observed from AVHRR during the study period. The researchers identified essential ancillary data sources to support this task, which is conventional to the inputs of other flood-mapping studies (Ali, Quadir and Huh 1989, Brakenridge and Anderson 2006):

- Physiographic and contour maps
- River system perennial water maps
- Previous flood maps (in (Rasid and Pramanik 1990), maps from 1954 and 1955)
- Supporting reports from local news papers

The color composite technique to determine water heights in (Rasid and Pramanik 1990) was supported by the use of a similar method in (Ali, Quadir and Huh 1989) combining brightness temperature and albedo to demarcate between the less turbid, lower albedo river water, and the coastal water with higher turbidity and albedo.

Visual interpretation similarly supports a commonly used method of density slicing or thresholding to find areas with water using a single-band approach (Frazier and Page 2000), by identifying reflectance bands with clear land-water separation and using a

threshold value that suits the scene or dataset. Like the previously mentioned use of the RED and NIR reflectance bands from MODIS and AVHRR, (Rasid and Pramanik 1990) used a color composite technique of the RED and NIR reflectance from AVHRR to classify the image (water bodies/deep flood, moderate flood, shallow flood, cloud cover, and land). As mentioned in (Ali, Quadir and Huh 1989), the red reflective bands are more useful for determining water turbidity, while the near-infrared wavelengths are more suitable for land-water boundaries, which makes combinations of red and near-infrared reflective wavelengths useful for mapping flooded areas. A method similar to the NDVI algorithm to detect healthy vegetation, there are two Normalized Difference Water Indexes (NDWI) that use the same formula as NDVI, yet instead use NIR and the short wave infrared (SWIR) bands (Gao 1996), and GREEN and NIR in (McFeeters 1996) as follows:

$$NDVI = \frac{NIR - RED}{NIR + RED} \qquad NDWIgao = \frac{NIR - SWIR}{NIR + SWIR}$$

$$NDWImcfeeters = \frac{GREEN - NIR}{GREEN + NIR}$$

Where the absorption of water in both SWIR and NIR bands are negligible, (Gao 1996) originally created the index to sense changes in vegetation canopy water; in contrast, (McFeeters 1996) used the green reflectance band particularly for the measurement of open water and turbidity studies. While the band combinations differ for both NDWI studies, both have proven to be useful to sense the presence of open water (Chen, et al. 2013, Guerschman, et al. 2011). A criticism of McFeeter's method to delineate water

effectively in urban areas due to urban areas having spectral brightness decreases from green to the NIR wavelengths, thus yielding similar NDWI values motivated the creation of the Modified Normalized Difference Water Index (MNDWI) (Xu 2006). The modified method solves the problem of background noise and urban areas by replacing the NIR band with a mid-wave infrared band MIR (band 5 on Landsat TM-4/5) at with the range 1.55-1.75µm. The development of the modified water index focused on the spectral differences in between water, built-up areas, and vegetation in MIR. As reflectance in built-up and vegetative areas increase in MIR, reflection in MIR decreases for water.

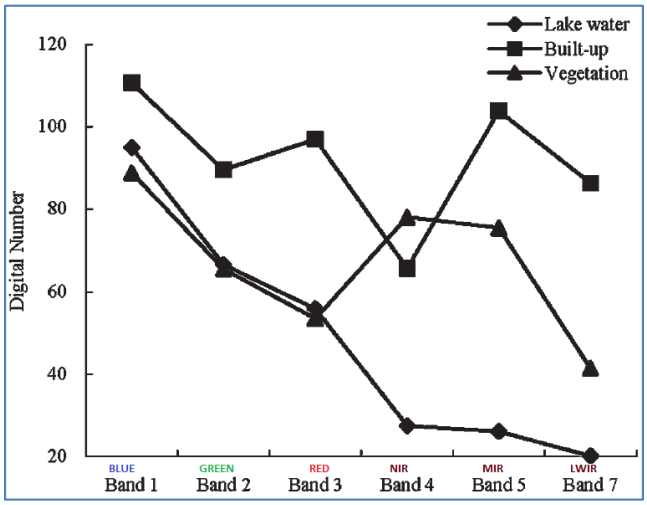

Figure 2- Reflectance for water/built up/vegetation -modified from (Xu 2006)

It is generally agreed upon that satellite imagery can be useful for flood detection, disaster response and mitigation, and prevention and warning (Brakenridge and Anderson 2006, Gao 1996, McFeeters 1996). However, the coarse spatial resolution can create issues related to classification where different land cover within close proximity within

the image pixel can create mixed pixels. In response to this problem, (Guerschman, et al. 2011) developed the Open Water Likelihood algorithm to quantify the fraction of the coarse pixels with standing water by combining the properties of NDVI, NDWI, and SWIR with an elevation model using the Multi-resolution index of Valley Bottom Flatness (MrVBF) (Gallant and Dowling 2003). Researchers in (Chen, et al. 2013) conducted a study that evaluated MODIS daily and 8-day products for floodplain and wetland inundation mapping, and used a specific index to detect water, the modified Normalized Difference Water Index, mNDWI and the Open Water Likelihood (OWL). MODIS 8-day composites are useful to alternatives to daily imagery that might have heavy cloud cover during rainy seasons; however, daily images have higher temporal resolution that is necessary for many analyses requiring high temporal resolution. The study concluded that there are negligible differences in the spatial and spectral accuracy daily and 8-day composite imagery for flood mapping and the composite imagery can serve as a replacement for daily imagery when cloud cover will regularly obscure the flood extent (Chen, et al. 2013).

While not the focus of the current study, the use of radar products has also become prominent in monitoring flood inundation and extent due to the ability for radar products to penetrate cloud cover. In (Töyrä, et al. 2002), researchers present the case that while satellite imagery in the visible and near infrared wavelengths are useful for mapping water extents, problems such as canopy cover and emergent vegetation can obscure and mix pixels, respectively, causing misclassifications errors. As (Töyrä, et al. 2002) used the satellite radar sensor RADARSAT and multispectral imaging sensor

SPOT data to create a composite to identify flood boundaries, (Ramsey III, et al. 2012) compared the usefulness of visible imagery from Landsat thematic mapper (TM) and Envisat advanced synthetic aperture radar (ASAR) system. Acquiring flood depth information can also be difficult to using visible imagery varying vegetation types or regularly flooded marsh areas (Rasid and Pramanik 1990, Ramsey III, et al. 2012). One solution to this was a comparison of cloud penetrating SAR and ASAR sensors in (Ramsey III, et al. 2012), which provided relative water penetration depths in different marsh areas in Louisiana.

Cartography of Flood Mapping

The cartography of flood mapping varies culturally around the world as well as by industry and domain. As scientists and planners in South East Asia, with limited communication with the product developers, will use the flood product in this study, it is important that the style and content display of the flood mapping product be consistent with cartographic standards in hydrology and flood mapping. A review of design methods and cartographic products for flood mapping and other real time disaster information from satellites is included in this section to help guide the use of color scheme in the final mapping product.

While there are many articles that explain flood mapping principles of cartography, many recent articles focus on the use of the internet to disseminate map information in an easily accessible way that is also user friendly (Carlson & Burgan, 2003; Gopinath, Ambili, Gregory, & Anusha, 2014), which applicable to flood mapping as well as other disasters such as fires and droughts.

In 2003, authors Carlson and Burgan reviewed users' needs in operational fire products (Carlson and Burgan 2003). Similar to the Flood Impact Product, the primary product in this article focuses on a MODIS 250 meter dataset to estimate daily fire danger. While the 'user needs' section of the article was dominated by the model input information, the authors strongly emphasized the need for high temporal resolution data to monitor the rapid change potential of fires. In most cases, easily accessible and user friendly information is disseminated through the internet (Carlson and Burgan 2003).

In (Roth, et al. 2014), researchers focused on the end-user to develop the NOAA Lake Level Viewer by first identifying user groups and creating user profiles for nine different user types. The nine profiles could be grouped into similar sectors for government interests, university/research, and industry users and by how the data would be implemented by end users. The Lake Viewer project tests six categories of symbolization by water level, with supporting categories of uncertainty and base maps. However, the product legend of low and high confidence used in conjunction with lake level proved to be difficult to interpret, as the majority of participants 14/18 indicated that the confidence legend needed to be explained more thoroughly (Roth, et al. 2014).

As mapping products are transforming from static representations to dynamic updatable formats on online databases, the cartographic expectations for mapping products shift based on user needs and the viewing capabilities of the website (Gopinath, et al. 2014, Carlson and Burgan 2003, Roth, et al. 2014). In the case of literature of flood mapping products and capabilities, the use of false color imagery (Chen, et al. 2013, Brakenridge and Anderson 2006) is prevalent, with separate depictions of flooded areas

without any backgrounds used to show extent. The false color imagery generally presents water as various shades of blue and black, where the darker color blue is deeper water (Brakenridge and Anderson 2006, Rasid and Pramanik 1990). Similarly, flood maps may use a natural color imagery with the delineated water bodies with a brighter blue color scheme to stand out from the imagery (e-GEOS 2011).

Flood maps created by Eastern researchers give insight into the cartographic style commonly seen in flood mapping in the east and Asia, and help to understand what the difference is, if any between eastern and western flood mapping conventions.

In the analysis of the accuracy of 8-day and daily surface reflectance for mapping areas in Australia, (Chen, et al. 2013) used a false color composite to begin the visual assessment of flooded areas, and stated that the darkness of the color blue in the scene was indicative of inundation and water extent.

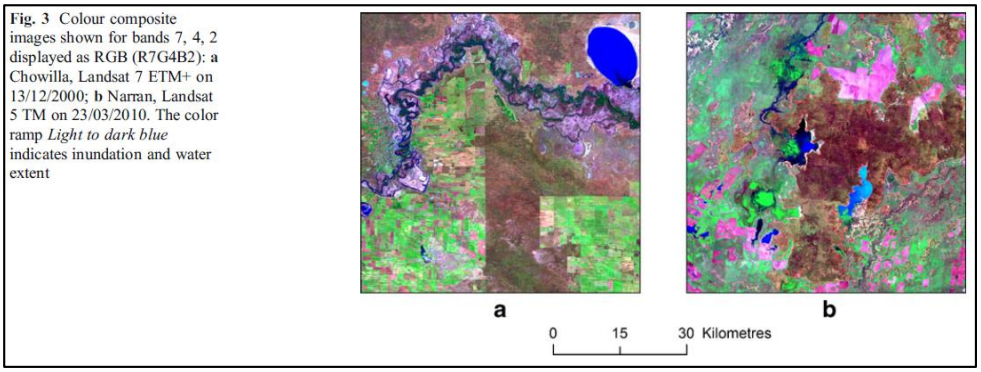

Figure 3- False Color Composite (Chen, et al. 2013)

Using the Open Water Likelihood (OWL) algorithm, OWL reports values from zero to 100, as the percentage of the pixel that has water. Using this technique, (Chen, et

al. 2013) suggested that all OWL values greater than zero were effected pixels, and therefore were classified as water. The color ramp presented depicts the percentage of the pixel inundated as shades of blue in four categories as follows:

2-10	11-50	51-99	100

Asia Insurance Review, a website dedicated to Asia's insurance industry featured a map illustrating river deltas in southeast Asia that are vulnerable to flooding, where the ocean bodies are white, the vulnerable areas are shown in blue, and the landmasses have natural color with topographic relief (Asia Insurance Review 2014). Because this map is targeted towards insurance specialists, and not necessarily scientists, the map focuses on labeling and highlighting the effected deltas, in a uniform color.

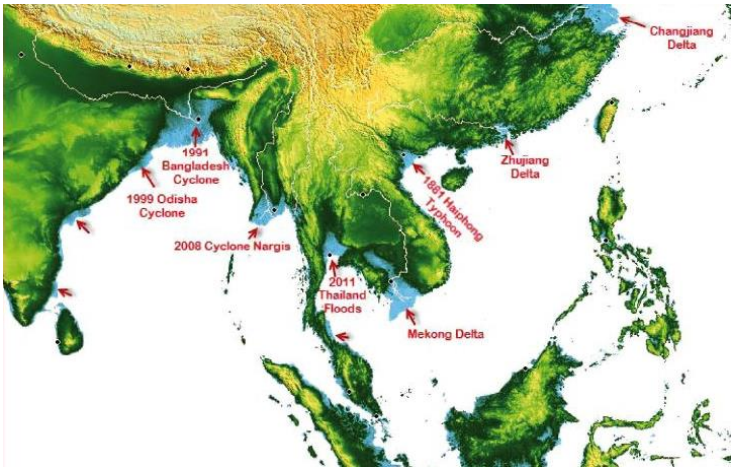

Figure 4—Asia Insurance Review Flood Prone Areas in Asia

In the Rapid Response Inundation Map Series by the Dartmouth Flood Observatory, (Brakenridge, Anderson and Caquard 2004) previously flooded extent pixels are shades of blue, while the newer effected areas are bright red. This pattern is also seen in a related project for global mapping in near real time (Nigro, et al. 2014), and is similar to the DEVELOP Flood Product, where the highest NDVI change pixels are orange and red.

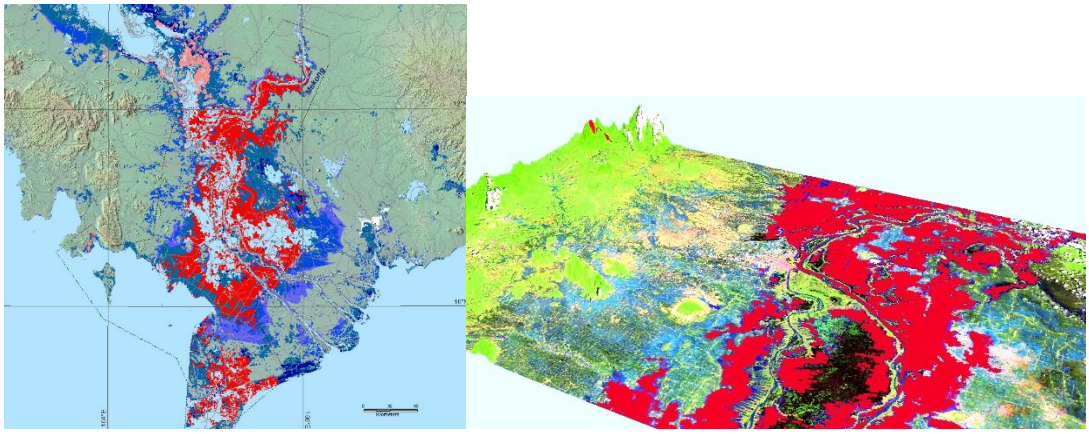

Figure 5—Flood Observatory (Brakenridge, Anderson and Caquard 2004) and DEVELOP Flood Product 3D Visualization (Doyle et al 2014) use red color scheme

Conclusion:

The Normalized Difference Vegetation Index (NDVI) is popular with many authors because of its ease of use by having a defined range of expected values falling between ± 1 (Sarp 2011, Wang and Qu 2007), and because the index presents less problems with scaling and noise than the Red/IR ratio method as observed by (Tucker 1979). The positive NDVI values generally correspond with healthy vegetation and values approaching 0.2 and below are generally considered unhealthy vegetation and

other non-vegetative materials (Myneni, et al. 1995, Pettorelli, et al. 2009). However, very few articles describe the implications of negative NDVI values outside the realm of drought monitoring as a primary study. Because NDVI is a vegetation index, and although NDVI scales between ± 1, the negative values that might imply features other than vegetation often go undocumented. However, negative NDVI values might answer questions to other environmental phenomena such as the presence of water, fire, minerals, or urban growth, yet these features are only explanations to the areas of low NDVI in otherwise highly vegetative areas. Put simply, values such as 0.2 through 0.9 are confidently referred to as the healthiness of vegetation, however, values such as -0.2 through -0.9 are not simply denoted as 'unhealthy vegetation' because while positive values all refer to vegetation, negative values refer to many different features. The assumption of subtly changing reflectance values due to physical change over time advocates the use of a range of acceptable values of NDVI outside of the mean before being classified as meaningful physical change.

Indices used to detect flooded areas are useful to the understanding of NDVI decrease values where there may not be flooding. While the current research focuses on using NDVI as an exclusive method to determine flood extent, future studies including additional algorithms such as OWL (Guerschman, et al. 2011) to determine how much of the pixel is inundated would be a useful addition to MODIS based flood mapping at coarse resolutions. Further, because flooding can occur in urban areas, the mNDWI index (Xu 2006) can support the delineation of NDVI decrease due to urbanization and the influx of water into the city.

As many authors support the use of layer stacking to product natural color and false color imagery, the use of such methods would be useful in the integration of the online web-based product, as the basemap imagery does not have the same temporal resolution of the new datasets that are used as overlays. Natural color imagery can support the flood extent product by providing a visual basis for users to compare area product with what the sensor is observing in true RGB color. While some studies use red and warm color schemes to symbolize the flood products (Brakenridge, Anderson and Caquard 2004, Nigro, et al. 2014), many flood maps use varying shades of blue for water, green for vegetation, and browns for bare soils.

RESEARCH METHODS

End-users to scientific products might not have the background knowledge to understand how the product was created, and therefore might not understand the limitations and capabilities of the product. Associating meaningful information and commonly used language in image classification is important to helping users navigate, and to get the most benefit from the product. To do this, a comparison study of the NDVI values relative to their respective land cover classification for each of the input scenes for the baseline image will be completed. This understanding of the expected NDVI values at each land cover class and each pixel location will guide the implications for anomalies at those locations similar to the method in (Gopinath, et al. 2014). The land cover dataset will come from the most recent (2012) MODIS product MCD12Q1, the Land Cover Type Yearly 500-meter grid.

Once values for the baseline image are understood, the NDVI anomaly can be classified into meaningful, qualitative classes. Based on initial visual assessment, the scale might be streamlined into four sections: Cloud/No Data, Not Flood-Dry, Not Flood-Wet, and Flood-Standing Water (Rasid and Pramanik 1990), or into sections that have implied meaning based on the color ramp used (Gopinath, et al. 2014, Song, et al. 2004). The classifications schemes focus on the segmentation of data into categories, but do not change the data itself. A comparison of the classification methods (*the original classification, standard deviation, equal interval, NDVI decrease*) proposed in the reviewed literature might suggest an ideal classification scheme for this type of temporal study. While the

classification schemes used the in the literature were used to describe changes in NDVI for drought, deforestation, or land reclamation, the schemes are not necessarily indicative of those phenomena. Rather, the classification schemes are used as a visual aid to assess change in a quantity that is visually understandable and can be associated with other data. This study seeks to find which classification scheme or interval best defines area effected by flooding.

Baseline Image and Anomaly

For the completeness of the study, the baseline image will be regenerated in order to capture individual NDVI values from each scene, which is not available with the current composite image. The original baseline was produced from 8-day MODIS composites by using the MATLAB Time Series Product Tool to take the maximum NDVI value from to create 32 day composites, and additional smoothing and filtering to remove remaining clouds and noise to average the Terra and Aqua data sets. This product was provided to the DEVELOP team by Joseph Spruce, a science advisor for the team, and the producer of the original baseline. The baseline image will need to be recreated to calculate the standard deviation from the mean at each pixel for the standard deviation classification. The baseline will be recreated on this basis, however, the use of the Time Series Product Tool is unavailable for this study and therefore results from the other classification types are expected to be different than when compared to the original baseline.

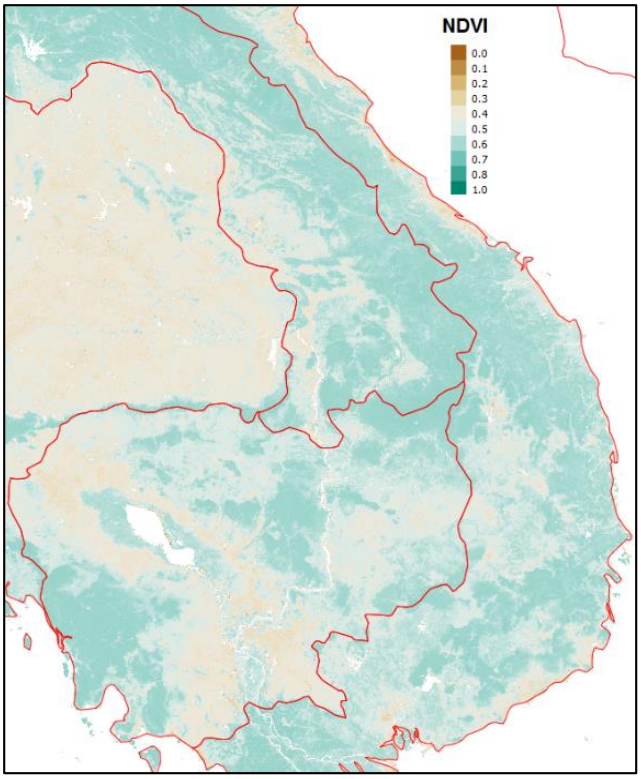

Figure 6. Original baseline

MODIS daily images (MOD09GQ-Terra/MYD09GQ-Aqua) will be used for the daily anomaly study, while 8-day image sets (MOD09Q1-Terra/MYD09Q1-Aqua) will be collected for each January in years (2003-2011) to create the baseline composite. The 8-day images will come from the MODIS sensor on the Aqua and Terra satellites. The MODIS images are downloaded from USGS Earth Explorer. Both Terra and Aqua satellites acquire local observations daily, at 10:30 am and 12:10pm respectively (National Snow and Ice Data Center; 2015). The baseline composite will be created using the 8-day composite imagery with the surface reflectance bands for the near infrared and red wavelengths. The 8-day image sets are derived from atmospherically corrected daily

images from the Aqua and Terra satellites to Level-2 processed quality. Masking errors from scan angles and poor observation coverage, the 8-day composite contains pixels from the best L2 (daily) observation within an 8-day period. These pixels are chosen based on absence of clouds, high coverage, low view angle, and aerosol loading. While these 8-day images have less obvious errors, the surface reflectance dataset provides band reflectance for the NIR and RED wavelengths, as well as the supporting quality information to identify remaining errors (U.S. Geological Survey; U.S. Department of the Interior; 2014). In addition to the removal of pixels identified as poor quality by the QA dataset, the pixels containing clouds will also be removed by taking abnormally high values in the RED wavelength. Most of the landmasses with the exception of inland water are free from errors represented by the quality band. The 8-day scenes form Aqua and Terra will be averaged into a final baseline product, while omitting pixel observations of poor quality.

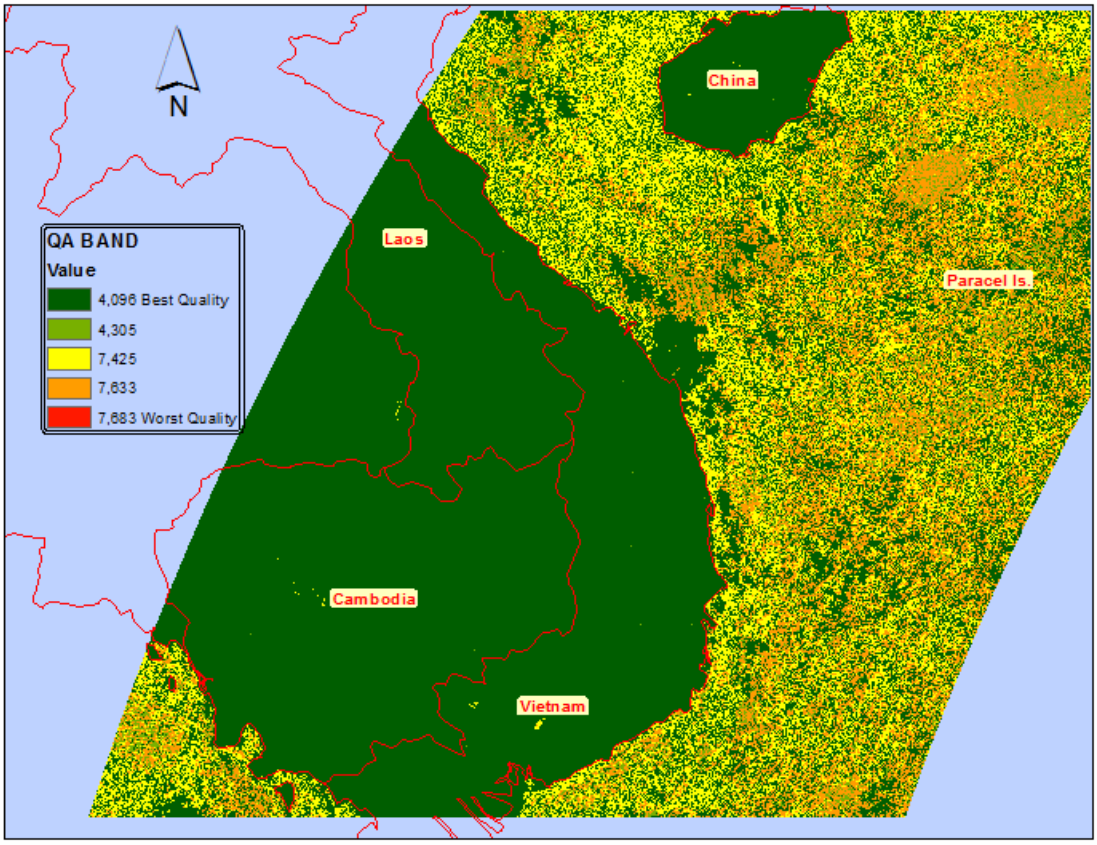

Figure 7. Quality Band example MOD09Q1- January 1, 2001

Original Classification—Percent change (Murad and Saiful Islam, Drough Assessment using remote sensing and GIS in North-West region of Bangladesh 2011): As described in the literature on NDVI anomaly, the NDVI percent change classification calculated by subtracting the new image from the old image, dividing by the values of the old image, and multiplying that value by 100: $\left(\frac{(ImageNew - ImageOld)}{ImageOld}\right) * 100$.

While the classification scheme will remain from (Doyle, et al. 2014):

0	4	15	30	50	75	100+

Standard Deviation Classification: The standard deviation of the pixel values from the images that created the baseline will be attributed to an additional image. The use of the standard deviation information assumes a normal distribution of observations, and allows the observed daily images more flexibility in variance from the mean before being classified as wet. The daily images will be compared to the baseline image via the associated standard deviation image. By the following logic:

- *If DAILYNDVI <MEAN+SD and DAILY>MEAN-SD* If the daily image pixel is within one standard deviation of the mean
    - *Pixel= 1 Standard Deviation (called 1)* ***OR***
- *If DAILYNDVI>MEAN+SD and DAILY<MEAN+(SD*2)* If the daily image pixel is greater than one standard deviation but less than the max of two standard deviations.
    - *Pixel= 2 SD pos (called 2)* ***OR***
- *If DAILYNDVI<MEAN-SD and DAILY>MEAN-(SD*2)* If the daily image pixel is less than one standard deviation but more than the min of two standard deviations.
    - *Pixel= 2 SD neg (called -2)* ***OR***
- *If DAILYNDVI>MEAN+(SD*2)* If the daily image pixel is greater than two standard deviations
    - *Pixel= 3 SD pos (called 3)* ***OR***
- *If DAILYNDVI<MEAN+(SD*2)* If the daily image pixel is less than two standard deviations
    - *Pixel= 3 SD neg (called -3)*

The classification scheme therefore will have five classes, although the positive SD values are unnecessary for flood mapping, the positive values can be made translucent:

3 SD neg or less	2 SD neg	1 Standard Deviation	2 SD pos	3 SD pos or more

Equal Interval Classification using Percent Decrease (Abbas, et al. 2014, Murad and Saiful Islam 2011)*:* Using the percent decrease method, the new classification scheme can be split into five equal interval classes to represent how much of the area has changed. However, because the data is dynamic, an equal interval classification would have to be based on scale to 100% change, but may have to change based on the range of observed values.

<20	21-40	41-60	61-80	81-100

NDVI Decrease (Song, et al. 2004)*:* Similar to the Percent decrease method, the scale values may require dynamic changes based on the predicted and observed values. The scale used in (Song, et al. 2004) will serve as a foundation.

< -0.25	-0.25 to -0.1	-0.1 to +0.1	+0.1 to +0.25	+0.25

The presented classification schemes from NDVI decrease and equal interval guided the use of 5-class system.

The Daily L2 Product

The daily images are also downloaded from Earth Explorer and processed using the change methods described above. However, the current web-based product runs on a server that searches for new data from Aqua and Terra and processes it in real time, twice per day as it becomes available. The L2 product similarly has quality assurance information to help distinguish poor quality pixel observations due to cloud cover and oblique scan angles. The DEVELOP real-time product currently does not integrate the quality assurance information into the product focusing on the removal of cloud cover, and therefore may have erroneous pixels affecting the outcome of the NDVI change analysis. Using a pixel based threshold technique, areas with pixels that reflect very highly in the red wavelength (derived from the 250-meter MYD/MOD daily product) are removed from the NDVI percent change product, and the data from the previous eight observation(s) from Aqua/Terra is used to back fill the removed pixels. This method has proved to be successful in the integration of

MODIS data at a high temporal speed of twice daily, while removing clouds and providing up-to-date information.

As the baseline image uses the information from the QA band, the daily observations will also integrate the use of the QA band as well as the iterative cloud masking composite technique.

Supporting data for anomaly detection

Because NDVI change can be a reflection of many factors as presented in (Nash, et al. 2014, Pettorelli, et al. 2009), supporting datasets from the Aqua and Terra MODIS daily 1-km fire product (MOD14A1) can contribute to the Flood Extent Product to filter out low pixel values associated with high and nominal confidence fires.

The 2012 land cover dataset will aid in making distinctions on NDVI decrease based on flooding or based on vegetation health (Gopinath, et al. 2014). The MCD12Q1 dataset (U.S. Geological Survey; U.S. Department of the Interior; 2014) provides five different land cover classifications for analysis of products with supporting land cover. The land cover classification scheme chosen for this analysis was the International Geosphere–Biosphere Programme (IGBP) classification (18 types) due to the complexity of the land cover types in the region. Using this classification is useful in determining NDVI decline due to urban reflectance changes. In addition, an association of land cover types with NDVI change will help guide future studies on NDVI decrease for those land cover types during the flood season. This study will take the mean change values for each anomaly date within the land cover class and compare them with the baseline mean and standard deviation

values to understand the difference between observed and expected values *(eg. The mean value in urban areas shows 80% decrease from the mean value in the baseline for August 1, 2014)*.

Permanent Water Mask

A new, local water mask will be created from the NIR inputs to the 8-day composite baseline image. It has been identified (Doyle, et al. 2014) that the currently used water mask (Carroll, et al. 2009) MOD44W could have affected the previous accuracy assessment since the permanent water has shifted in the past few years, and the supporting data from the SRTM that was used to create the product was acquired much earlier in 2001. To create the water mask from the composited imagery, the dark pixel values from the NIR band will be extracted as permanent water by at each scene and composited into a final water mask product. The extracted areas will each be output to new files with binary classification that will be added together into one scene. The resulting image will have pixel value ranging from 0, where none of the scene contributed to the image report dark values at that location, to 40, where all of the 40 input images report pixels having met the dark value criteria. Pixel values over with 66% of dark value observations will be considered permanent water in the final product. For example, where pixels for all 40 scenes are rated best quality by their corresponding QA band, if at least 27 scenes have the dark value observations, those pixels will comprise the final product. However, not all pixels will be rated with an acceptable quality rating for each scene, and therefore they will be omitted from the calculation. Future studies will discuss the temporal relevance of elevation models and hydrological modeling input variables.

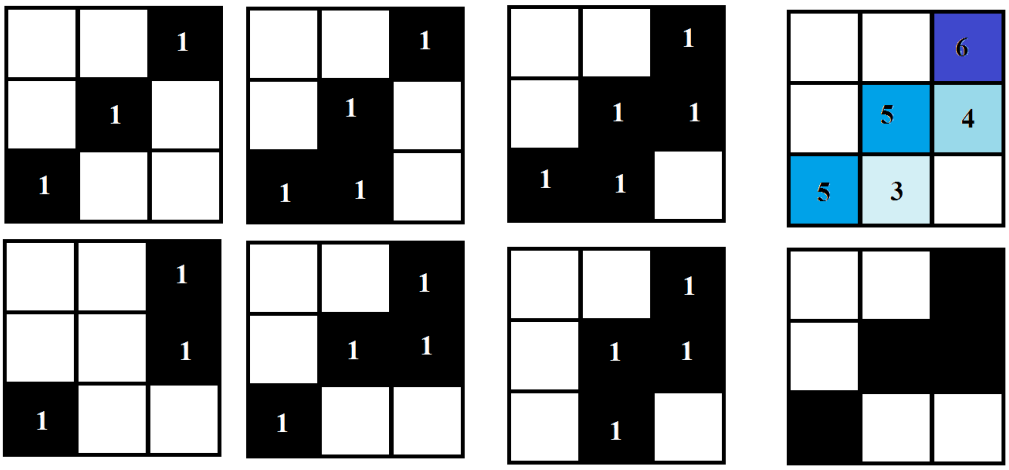

Figure 8. Pixel Threshold Based Water Mask

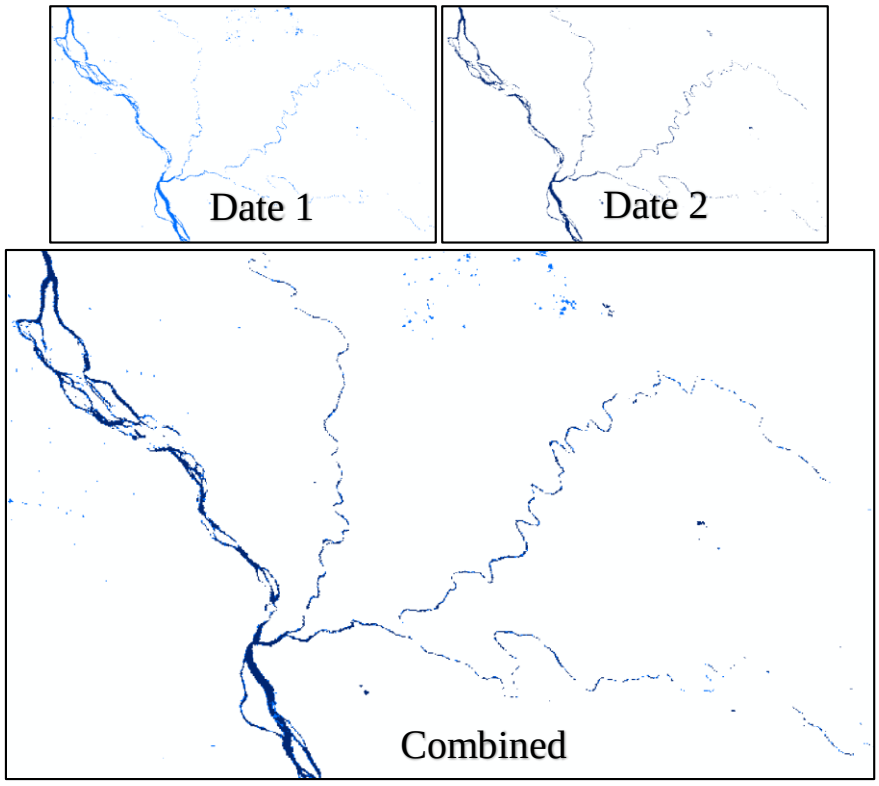

Figure 9. MODIS Water Mask Creation with NIR

Final changes to the product legend will be determined based on the reclassification comparison and accuracy assessment with Landsat imagery. The assessment of the four classification schemes will be completed by dividing the NDVI anomaly classes into distinct files to be compared with Landsat imagery for the same date.

This research will not interfere with the existing Flood Dashboard products and data acquisition scripts, and data will be acquired manually over a subsection of the study region, primarily in Cambodia and Vietnam, with only one MODIS tile. The product featured on the website may be modified with successful results of this research.

ANALYSIS

New NDVI Baseline and Water Mask

To complete the study, the baseline NDVI scene was recreated. However, because of limitations of available software and programming abilities, the baseline was created with the same data inputs, and with slightly less processing. The original baseline NDVI was produced from four 8-day composites from Aqua and Terra for each January from 2003 to 2011. The composite scenes were combined using the MATLAB Time Series Product Tool (TSPT), where the QA band and other inputs were used to remove sensor data irregularities. The TSPT interpolates between the omitted observations to create a smoothed distribution of NDVI for each pixel. The maximum NDVI for each pixel is assigned from the 8-day smoothed NDVI inputs to create a 32-day composite. The 32-day composites are averaged into the final baseline with additional noise smoothing.

The new baseline also uses 8-day composites from Aqua/Terra MODIS, and is processed using the R Statistical Programming Language. The near infrared, red, and quality bands from each of the 8-day images from Aqua or Terra is read into R and transformed into matrices to calculate NDVI. The "best" quality, value 4096 is compared with each of the dates, where pixels that do not meet the quality standard are not included in the overall calculation. In addition, the red band is used as an extra step to remove clouds that are still present after the initial surface reflectance processing to L2 quality. In the clouds area considered visible in the red wavelength at reflectance values above 2500 for the purpose of this study, this value was applied at the same stage as the quality

assessment. To take the mean NDVI over all pixels excluding the poor quality and cloud observations, three additional matrices were created to count the values of each useable observation in the red and infrared bands, and the amount of times a value that location has been accepted into the baseline. After all of the images from Aqua and Terra are combined into red and infrared totals, the mean NDVI was calculated as the fraction of each band over the total of observations at that pixel location. In few rare cases, the denominator will be zero, as there may be no ideal observations for that pixel, making the division by zero yield a NULL value. Those pixels will be converted into "-2", as a value clearly outside of the possible NDVI range, and therefore easily identifiable to be ignored in the processing of anomaly data.

Because of differences in how the baseline images are processed, it was expected that there would be differences between the baseline products. Specifically, because of additional processing of no data interpolation and noise reduction in the original (Spruce) baseline, the baseline was expected to have a more narrow range of NDVI values than the new baseline, which was created solely by masking out potential clouds using the red band, and pixels with low QA assessments. The new baseline does not use any interpolation between missing data, and therefore some pixels have more usable observations than other pixels. Having variable numbers of observations across the scene introduces a sample bias, which may be apparent in the product. The anomaly classifications used in this study have been created with the Spruce baseline, and the new baseline. The new baseline was created primarily for the purpose of using the standard deviation classification method, and therefore the Spruce baseline is not available for that

classification. The figures in the body of the text refer to the new baseline. Figure 10 and Table 1 below explain the geographic differences between the baseline products, as well as the cumulative differences between the products.

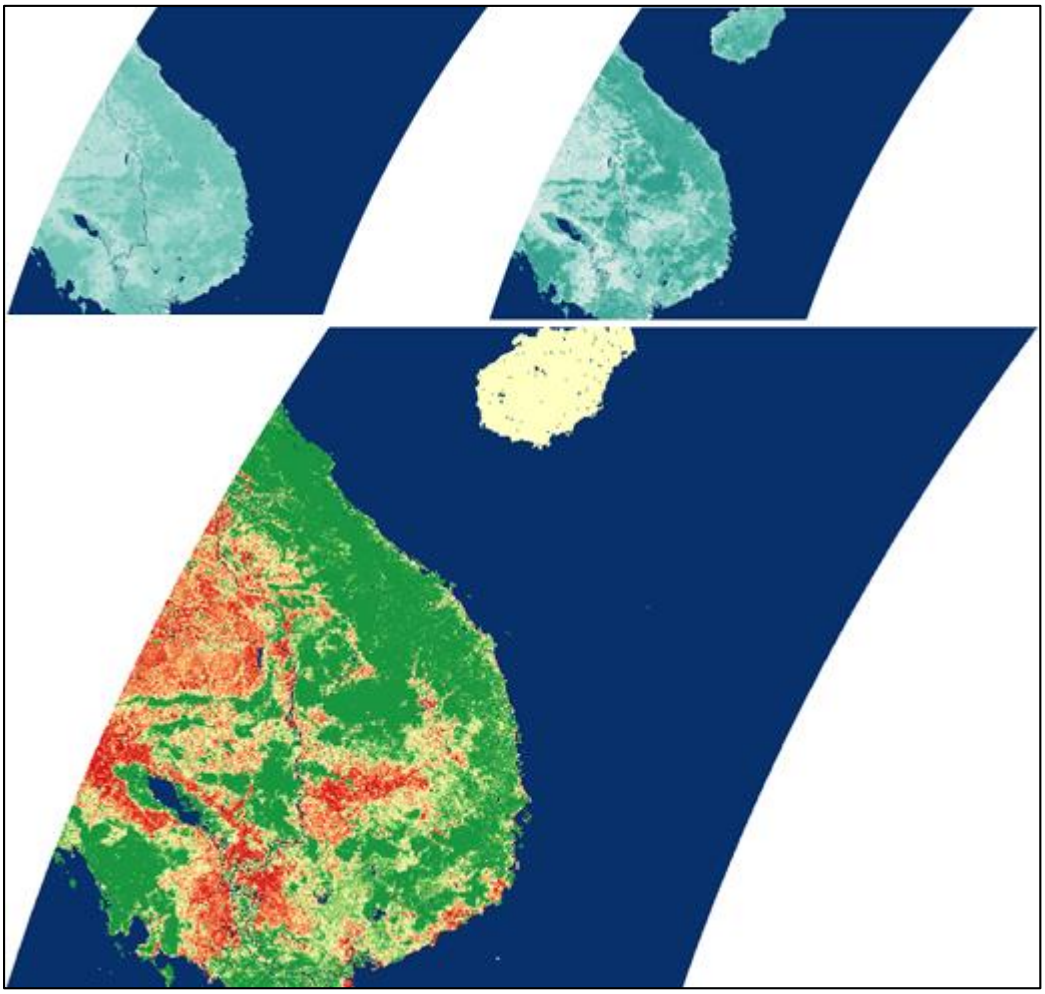

Figure 10 Left Top: Original Baseline Right Top New Baseline. Bottom Center is the difference.

Table 1. Baseline Image Statistics

MIN			MAX			MEAN		
SPRUCE	NEW	DIFFERENCE	SPRUCE	NEW	DIFFERENCE	SPRUCE	NEW	DIFFERENCE
0	-0.03355	-0.5575628	0.73	1	0.7	0.219682	0.237816	0.01813464

Updating the water mask for use in this study was important for the temporal relevance of the flood anomaly products. As has been discussed (Nigro, et al. 2014, Doyle, et al. 2014), the MOD44W product is becoming outdated, which can influence the accuracy of mapping floods relative to the permanent water bodies. As the MOD44W flood product was published in 2009, years of flooding over time can cause terrain changes and the addition of new inland water bodies (Carroll, et al. 2009). In this study, six years have passed since the creation of the MOD44W and the increase of flooding in recent years has made new water bodies, evidenced in the new water mask.

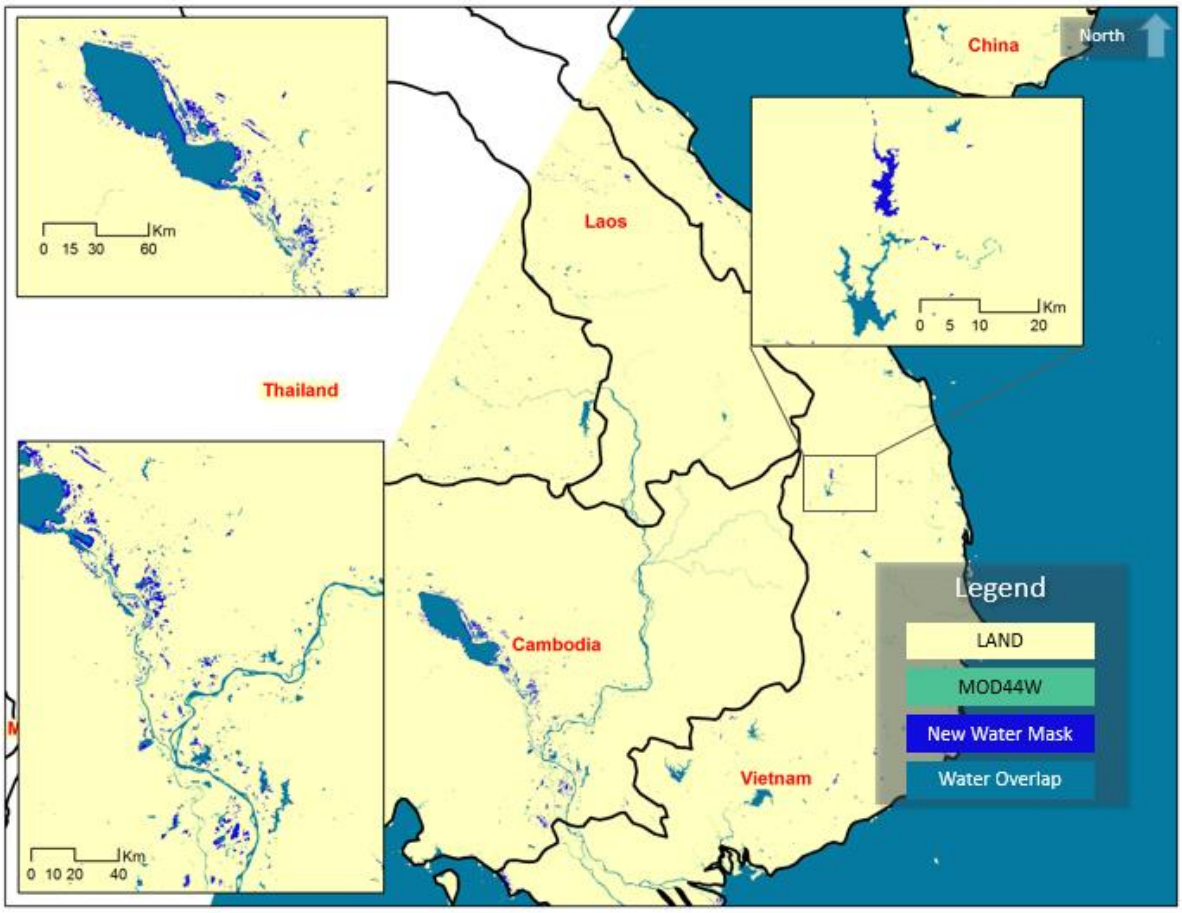

Figure 11 water mask comparison.

The original water mask MOD44W product is a global raster dataset at 250-meter resolution. The product came in response to the lack of available water raster datasets for use in remote sensing applications at a fine scale; the authors cite eight vector and raster datasets with resolution spanning 90 meters to 110 kilometers (Carroll, et al. 2009). The majority of the available datasets for mapping inland water have a resolution of 1 kilometer, with the exception of the Shuttle Radar Topography Mission (SRTM) Water Body Detection (SWBD) product at 90 meters. In addition, the authors cite the temporal relevance of products having been produced from 1999-2005. The global raster water

body dataset MOD44W was created by combining optical data from MODIS, SWBD, and the Mosaic of Antarctica (MOA). These datasets were combined in three sections of latitude based on the product availability and clarity, as the SWBD product does not extend to the poles, and the extent of MOA is 60° to 90° S (Carroll, et al. 2009). Within the study area of South East Asia, the MOD44W product relies heavily on the SWBD as a base, with MODIS 250 reflectance data to fill in gaps. The SWBD was chosen to create the MOD44W water mask from 54°S to 60°N because of its fine spatial resolution and the ability for the radar product to penetrate clouds and have a clear view of surface properties (Carroll, et al. 2009).

The new water mask proposed for this specific study area is not in response to errors in the original dataset or how MOD44W was created. Instead, the new dataset focuses on the temporal accuracy in order to determine flooded areas in recently acquired imagery fairly, and is only created for the one MODIS tile in the study area, unlike the global MOD44W product. The MOD44W MODIS input information was derived similar to the new water dataset, where the number of pixel observations and a percent of those observations being considered water are assumed water. Although the anomaly dates are current, the new water mask and the baseline NDVI product are not fully up-to-date as they are both created with the same years as the original NDVI product from Spruce with data MODIS surface reflectance for 2003-2011.

There are 72 input images from Aqua and Terra during this study period used for the baseline NDVI and the water mask. The new water mask was created solely with the dark reflectance values from the infrared band, where water is assumed to have a

reflectance of 1000 and darker. Similar to the baseline NDVI creation method, the red and infrared reflectance images are read into the R Statistical Programming Language as matrices and the pixels matching the reflectance criteria are added into one composite matrix. Initially, water had to be observed 66% of cases to be considered in the final water mask; however, that requirement proved to be too restrictive and eliminated many water bodies and river segments due to poor quality by the QA band or by cloud interference. Instead of enforcing the 66% criteria, the method required only 24 observations per pixel to be accepted in the final mask. This change also proves useful where new water bodies have formed in the past few years, when 24 observations between Aqua and Terra means 12 observations per sensor and 4 observations per year requires that the water only be present for 3 years at the very least.

Because the new water mask is based on reflectance and no additional datasets, it is likely to miss some areas of rivers due to areas where rivers narrow or have small islands or islets, and the spatial aggregation can transform the entire pixel into 'land'. While this might be viewed as a drawback, the possible flooding of these areas during the wet season may fill the gaps in missing pixels to show a more pronounced river. The water masks are shown overlapping in figure 11 above, where the MOD44W is stacked above the new water mask, and there is a newly identified water body shown in the image subset in the upper right corner of figure 11.

Figure 12 highlights the areas that are dissimilar between the two datasets. The green areas are new water areas, and the red areas are from the MOD44W dataset, which are not included in the new dataset. It is visually apparent that the new water body dataset

is particularly suited for larger water bodies due to the coarse resolution, while the MOD44W water mask uses a 90-meter input, which can detect smaller water bodies particularly where smaller rivers feed into the Mekong River. Of the number of pixels in the area, 74,777 pixels differ; concluding a .3245% difference between datasets, and an overall 'water' pixel increase of 1899 pixels at 250-meter resolution means a 474.75 kilometer^2 increase in surface water.

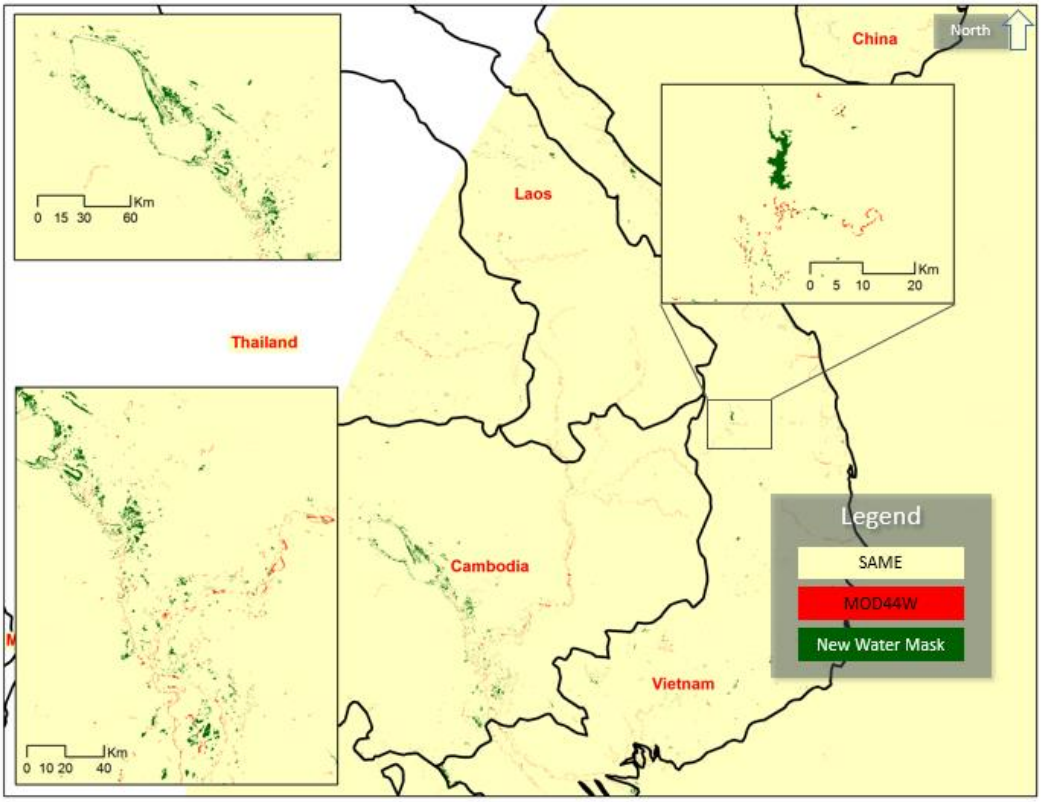

Figure 12 water mask difference

Daily Composites

The method used to create the twice-daily composites came from the original DEVELOP project, where the author of the present study created a method to combine observations from the Aqua and Terra satellites into 'moving window'-type products. The method was created after weeks of experimentation with moving window algorithms, averaging, and value prediction to increase the temporal resolution of the DEVELOP Flood Extent Product. Previously, the flood extent product utilized an average from Aqua and Terra 8-day observations. This was clearly a problem for the 'near real-time' nature of the flood product, because the product would update after every 8-days. The perception of 'near real-time' also gave the expectation that the map would update near the same temporal rate as the flooding occurs. The 8-day observation time was an obvious improvement to static flood maps that are created in emergencies, but rapid changes in surface processes could not be viewed, and in the event of sudden increase in flooding, the map became obsolete within two days of updating.

The end-users for the DEVELOP Flood Extent Product are primarily the Mekong River Commission (MRC), who manage and maintain the river and the river basin. Currently, the MRC utilizes a Near Real-Time River Monitoring Map that updates the status of gauge stations along the Mekong River and its tributaries every 15 minutes. To complement the water level information from the River Monitoring Map, it was proposed that the latency of the product be shortened from eight days to two days or less.

The 8-day product was originally used because of cloud cover in the scene obscuring the view of flooded areas. The figure below shows four days of consistent cloud cover over the study area from Terra during the month of August in the middle of monsoon season. These four days, as well as the same four days for the Aqua are composited into a 'current' scene. This same process was completed for four days at the end of May, the beginning of the monsoon season, and four days at the end of November, the end of monsoon season.

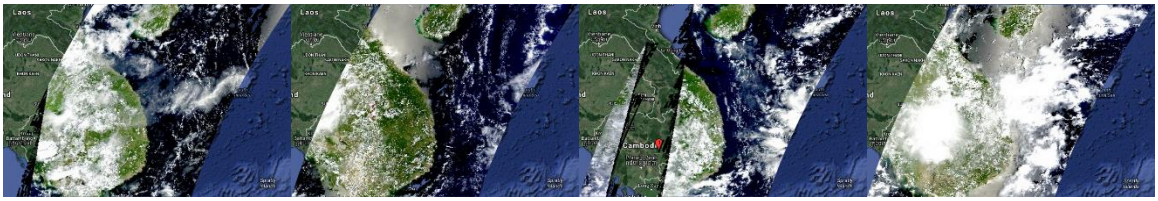

Figure 13 August composite scenes (from left, August 22→August 25)

Because of missing data stripes and persistent cloud cover, the use of daily images and image averaging was impossible. Instead, the images were stacked in order from newest to oldest, with the newest image taking the most precedence. The processing for these images was conducted in R Statistical Programming Language. For the Online Flood Dashboard, Aqua and Terra images are downloaded from the Land Atmosphere Near real-time Capability for EOS (LANCE) NDVI is calculated over each scene. The daily NDVI images along with associated red-band reflectance is then processed to into a "for-loop" logic, where the red-band reflectance values over 2500 are used to mask out

clouds in the corresponding NDVI scene. Areas with no data values are also removed in favor of the image preceding the most current image. The values are assigned in each image by transforming no data zones into a -300 fill value, and no data for NDVI are filled with -2. For each new composite, each row and column are selected to identify exact pixel locations. For each location, if the red band pixel reports a less than 2500 and greater than -100, and the NDVI pixel reports a value greater than -1.5, and the quality band pixel reports a good quality value of 4096, then that the NDVI pixel is considered acceptable, and can be incorporated into the twice daily update. If not, the previous observation at the same location is searched. This loop continues for each pixel in the scene for a maximum of eight observations, four days. If after the end of the four days the pixel has not found an appropriate match the pixel is given a 'no data' or cloud fill value, shown in the top layer of figure 14.

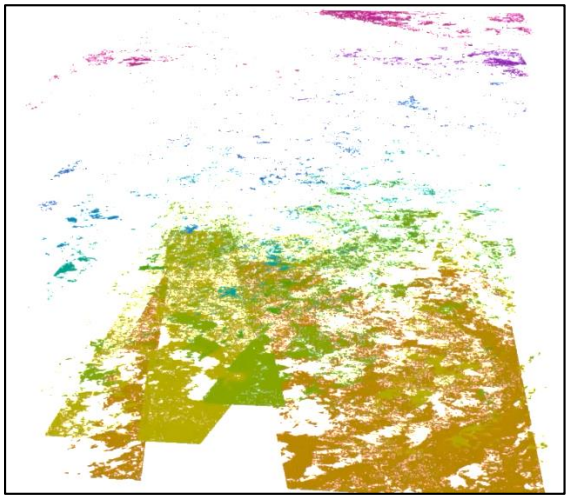

Figure 14 pixel stacking method

The process continues twice every day, as the R-script looks for new data on the LANCE server, and processes it into a new image twice every day. For this study, the images are downloaded manually from EarthExplorer, and only one image in May, August, and November are demonstrated. Figure 15 below shows the NDVI composite for the mid-monsoon season observation, with data from August 22-25.

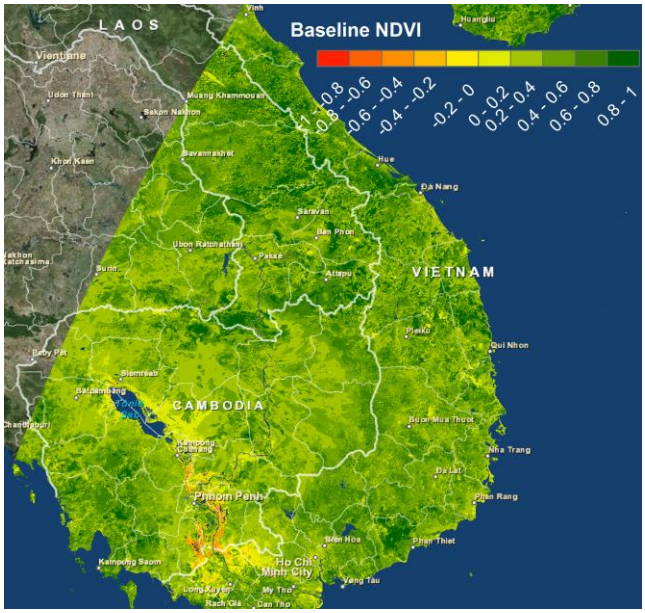

Figure 15 August NDVI: Note the area to the east of the Tonle Sap Lake appears slightly fuzzy or smeared. This is due to haze and thin clouds that are not fully masked. Future updates to the compositing system will incorporate the MOD35 Cloud mask.

Change Methods

To monitor change over time, two methods are particularly common: monitoring the rate of change in percentages, as well as computing the difference between the images

keeping the units of measurement from the original datasets. The percent change method is particularly popular because rate of change is generally understood; however, identifying a particular threshold for an alert to signal a major change, or the presence of the phenomena being measured is particularly difficult. Because setting a threshold for values of interest can be difficult, the meaning of the percent change values associated with the product are meaningless. The subtraction method is also widely used for in change detection in remote sensing.

In (Spruce, et al. 2011), a minimum 4% NDVI decrease threshold value was used to determine areas that were defoliated by moth infestation. The 4% threshold is unique to the study in order to apply coarse resolution MODIS imagery to physical changes that occur as much finer scales. The 4% threshold in (Spruce, et al. 2011) might otherwise translate into a 20% change or greater when using a finer spatial resolution product. Due to mixed pixels over large forested areas, the 4% threshold is useful for monitoring slight changes in defoliation.

On the other hand, (Murad and Saiful Islam, Drough Assessment using remote sensing and GIS in North-West region of Bangladesh 2011) used a minimum 1% NDVI decrease threshold to monitor drought, although the highest decrease classification stopped at 30% due to the predicted risk of the observations at the NDVI decrease locations in relation to meteorological values from Standard Precipitation Index. The most severe drought assumes an NDVI decrease of 30% in the Bangladesh study area.

In the literature search, there were very few articles that define an NDVI change value or NDVI range associated the with phenomena to be mapped. Using NDVI percent

change for mapping floods poses a particularly interesting challenge because of the assumptions that are introduced based on the physical characteristics of NDVI as well as the surface characteristics of IR and red reflectance. Presenting the equal interval classification of expected values from (Abbas, et al. 2014), and the original flood mapping product are shown below. These images contain the exact same values, but are symbolized differently based on flood mapping convention, and varying intervals.

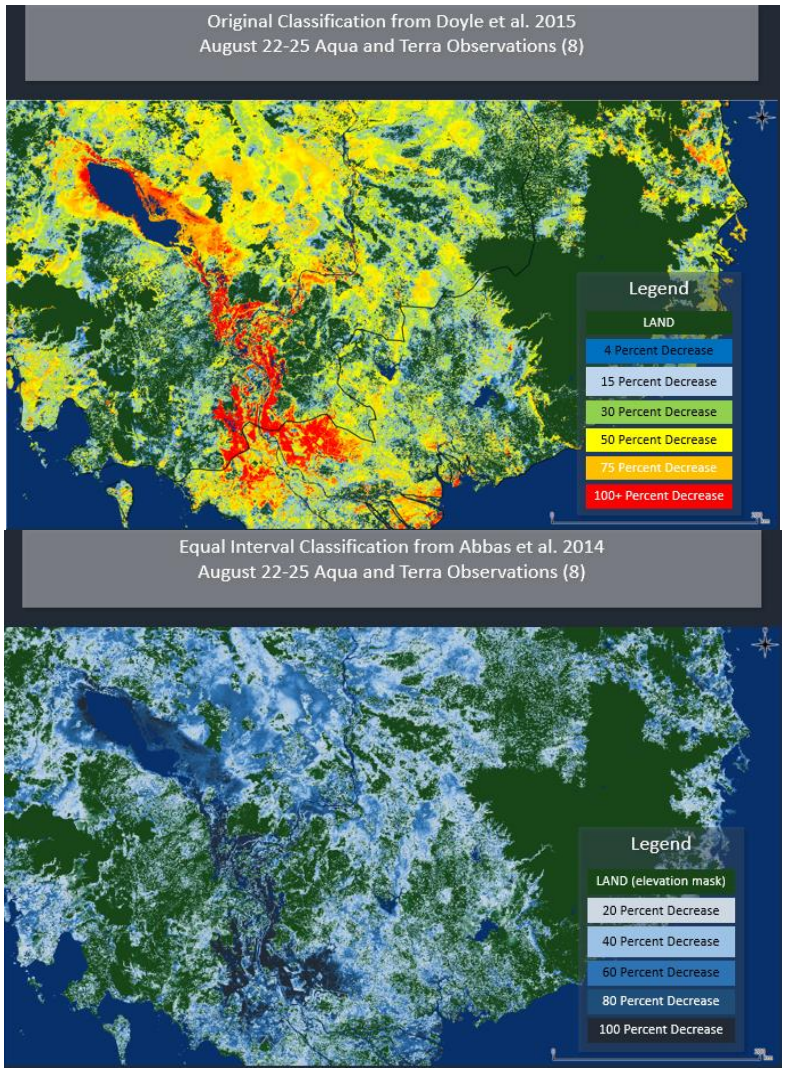

Figure 16 Top: Original DEVELOP classification Bottom: Equal Interval

What is immediately striking about the two is the color scheme used is the DEVELOP product's uses of unrelated colors to create distinctly different classes at each interval, while the Abbas classification uses a light to dark blue color ramp, which blurs the boundaries of each interval. In contrast, the use of distinct colors through the scene may be useful to distinguish between intervals, yet might still be confusing halfway through the color ramp when the values switch to yellow.

To create the percent change images, the composite images created in an earlier step are processed in R with the baseline NDVI with the percent change formula.

The application of the differencing method used in (Song, et al. 2004) depicts exactly how much change occurred at each pixel with the same units of measurement, which can be more simple to explain to users than unit changes and expectations for percent variations. This is also useful in the case previously mentioned, where low baseline values such as 0.02 can yield very high rates of change. The difference is also the easiest to compute where the baseline image matrix is subtracted from the anomaly matrix, and the product is converted back into a raster.

While the differencing method is useful for determining change, and finding decrease in NDVI, the problem of choosing an appropriate threshold still exists, and is domain specific. This study used the color ramp and interval classifications from (Song, et al. 2004), which was originally created to monitor drought areas. The classification shows that the interval ramp used in (Song, et al. 2004) is over saturated, and specific areas of change are difficult to distinguish.

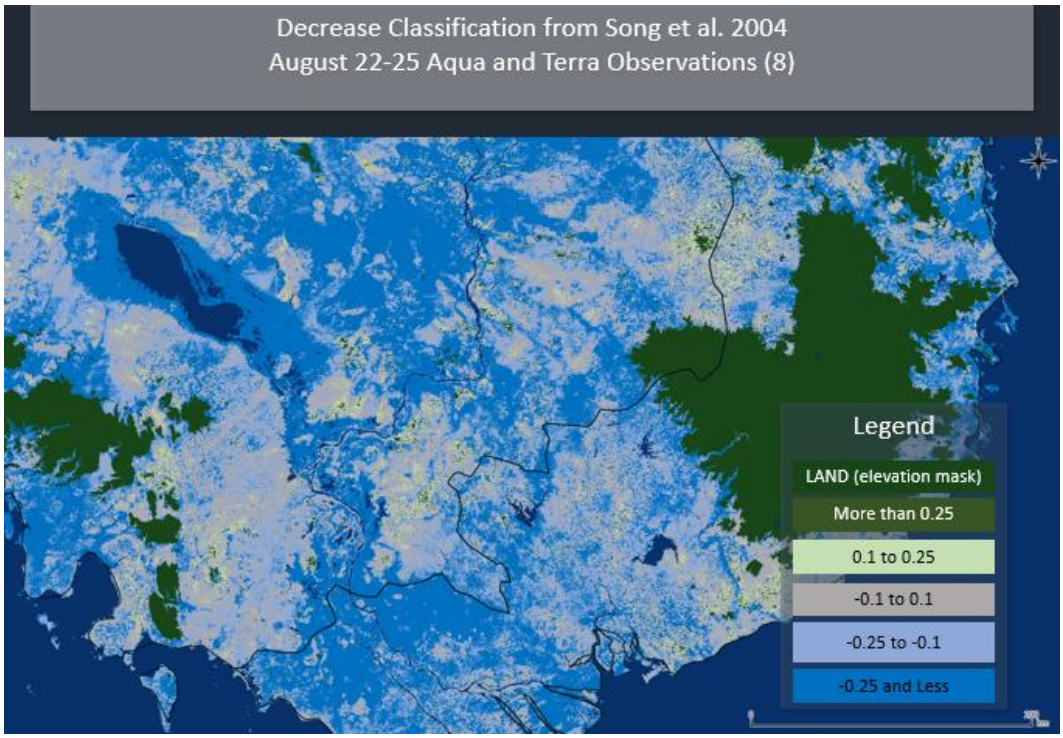

Figure 17. Song Interval Color Scheme

Another common statistical method to describe the deviation from an expected value is by calculating the standard deviation of the mean of observations. Using standard deviation produces an expected a range of values in relation to the mean observation. Tracking the increase of vegetation in a former mining area (Sarp 2011) visualized change from 1989 to 2000 ± one standard deviation. Using the standard deviation would be applicable in this case to reduce noise caused by slight variations from a mean value. The standard deviation classification allows greater movement within each standard deviation without the area automatically being flagged as 'changed'. This is important to consider when there are eight years of observations to create the baseline, and the terrain

may change slightly over time within each January—it is possible to detect percent change and NDVI decrease in the January twice-daily observations of the current year. Slight changes have the potential to overestimate flooding when all decreases in NDVI are considered flooded.

The Standard Deviation classification required more processing than the simple percent change formula or the simple subtraction, as this classification requires an additional dataset, a raster representing the geographic standard deviation of NDVI in the study area. While R Statistical Programming Language is primarily for calculating statistics, certain functions such as calculations of a group of raster images can take hours or days to complete, depending on the number of pixels in each image. There is a function to calculate the standard deviation of a raster stack, but because of time constraints, the standard deviation was calculated manually. The baseline image is used as the mean to compute the variance from each of the 72 8-day baseline input. After all of the images are converted to matrices and computed into the variance matrix, the square root of the variance matrix is taken to create the standard deviation matrix, which is converted into a raster.

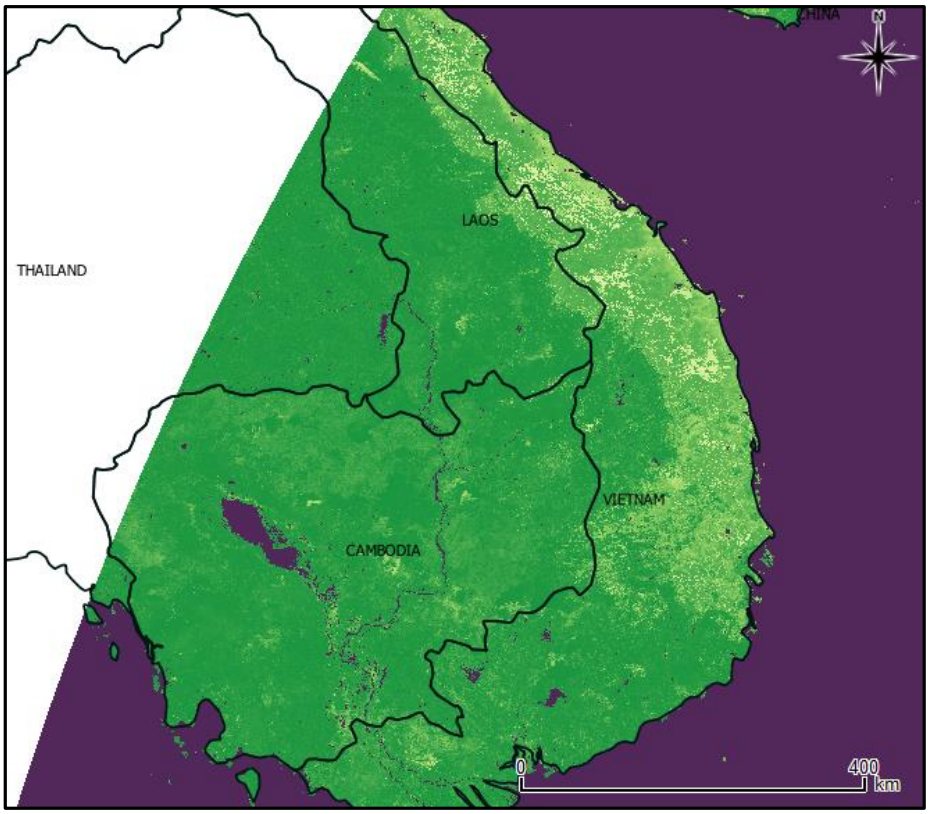

Figure 18. Standard Deviation Raster

Processing the daily images with the standard deviation classification required a logical formula to calculate which standard deviation class the pixels belonged. To process this classification, the daily image, baseline mean, and standard deviation from the mean rasters are read into R and transformed into matrices. For example, in each cell in the daily image matrix, if the value of the cell was less than the mean plus one standard deviation, and more than the mean minus one standard deviation, the value of the anomaly classification would be given 1, for one standard deviation. This process continues throughout the scene for ±3 standard deviations.

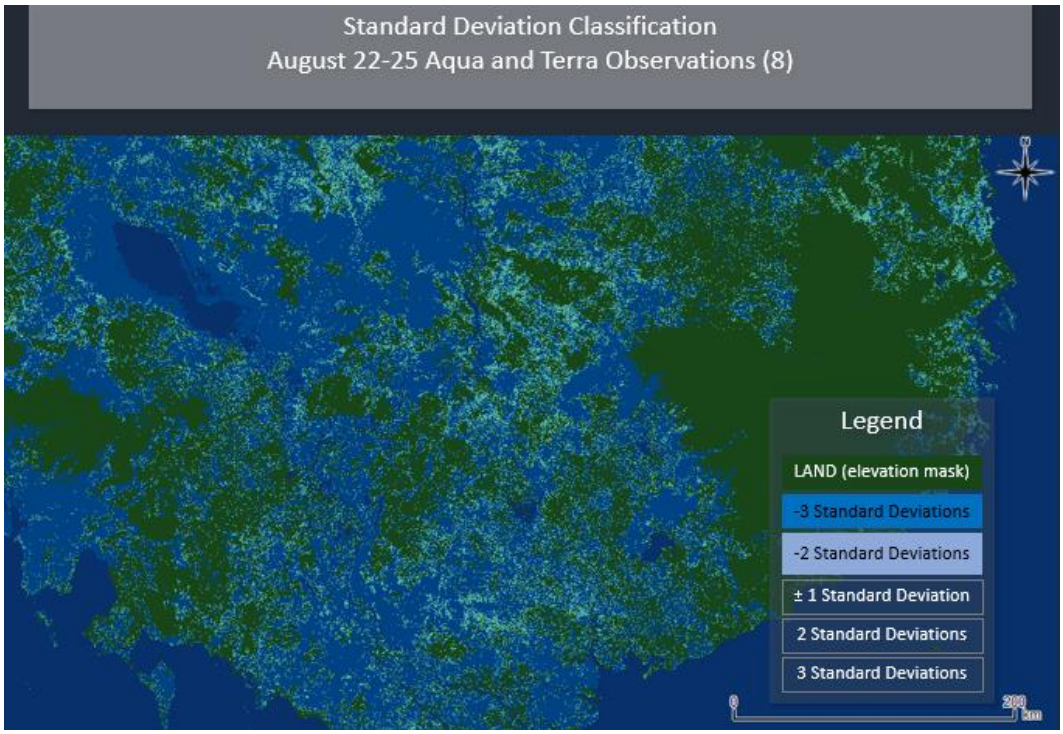

Figure 19. 1-3 Standard Deviation Anomaly Classification

Using one standard deviation from the mean unsurprisingly did not present any real evidence of flooding, particularly because it merely reports values similar to the baseline image. Therefore, three or more standard deviations from the mean, which is far beyond the expected values for January, were calculated using the same logic.

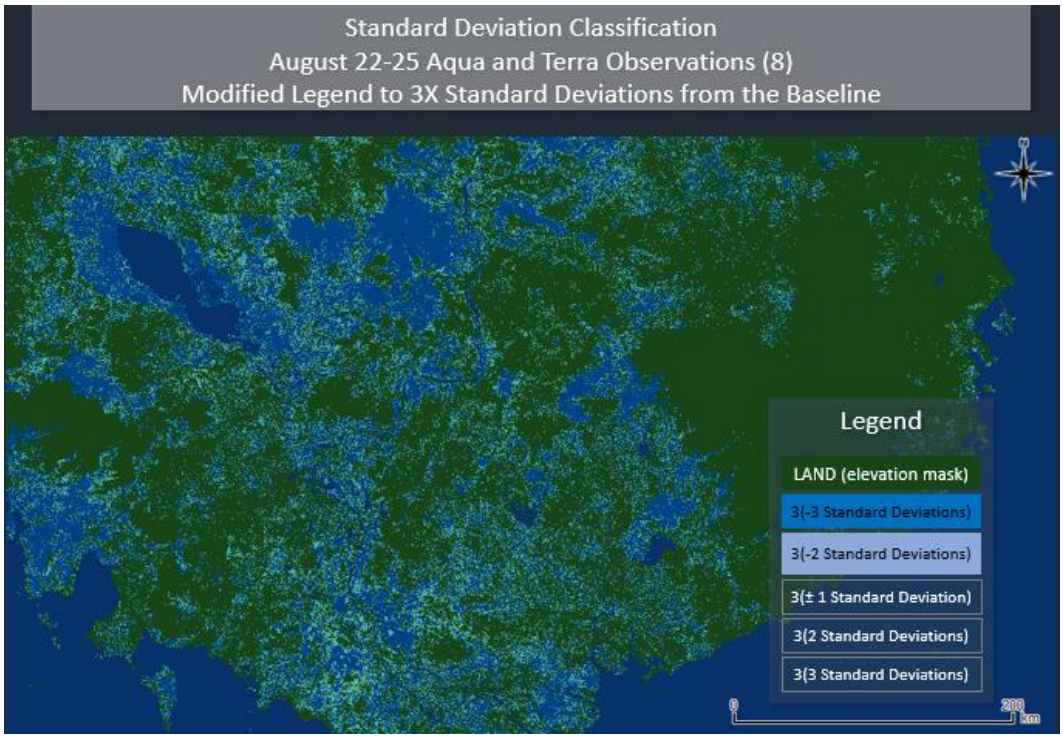

Figure 20 3, 6, 9 Standard Deviation Classification

The idea of using more than three standard deviations is confusing to most because generally standard deviations are referred to in terms of 1,2, or 3 standard deviations from the mean, or in cases with minor changes, half and quarter standard deviations can be used, and is a standard classification option in ArcMap. When three standard deviations encompass 99% of expected values for the January baseline, values falling within three standard deviations could have occurred in the month of January, and to observe values falling within the norm is not worth nothing. Using more than three standard deviations looks for values that are abnormal for January, reducing effects of small amounts of variation that is possible within the dry season. Using more than three standard deviations requires that the data bear very little resemblance to the original

dataset, as it is expected that the surface properties of land in August would not resemble the surface properties of January. Using this method should eliminate reports due to small variations of land surface due to seasonal effects, and focus on areas that are highly dissimilar from the January baseline image. This idea can be explained in a calendar format, where we expect a certain range of NDVI values from each month. If the a 'baseline' were calculated for each of the 12 months, there would be a frequency distribution for each month; August values might be several standard deviations away from the January values. Values deviating from one month might better characterize another month, as extremely low NDVI values are completely probable for August, but unlikely for January.

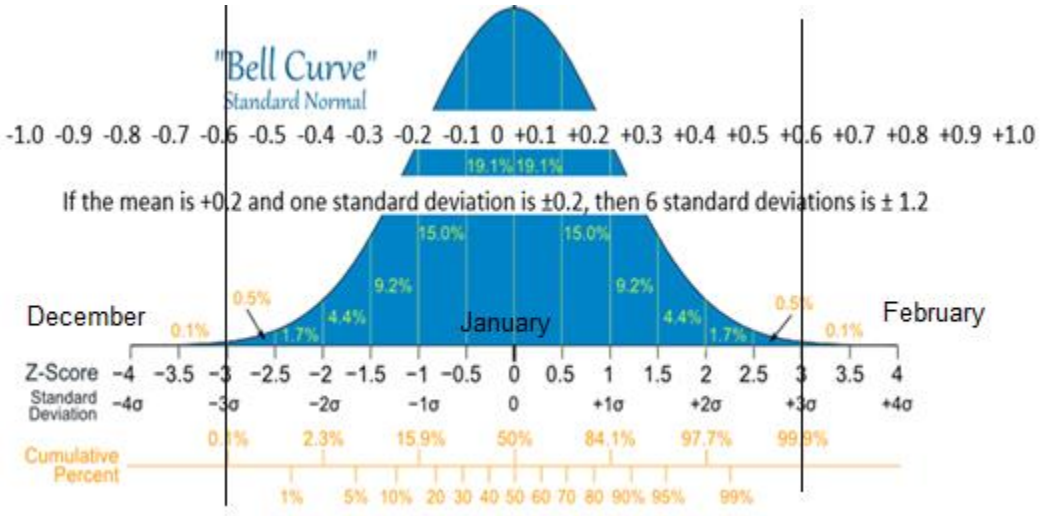

Figure 21 Bell Curve (modified from Mathisfun.com)

Land Cover IGBP and Fires Product

Land cover datasets are commonly used as supporting information or a principal analysis datasets in remote sensing of land surface processes (Gopinath, et al. 2014, Murad and Saiful Islam, Drough Assessment using remote sensing and GIS in North-West region of Bangladesh 2011). The analysis of land cover can vary relative to the type of study and the importance land cover has relative to the datasets. In addition, because land cover can be characterized in many ways, and derived from various datasets, the type of land cover classification product and temporal relevance is important to relate surface characteristics to the principal data of the study.

For this study, a MODIS georeferenced 500-meter land cover classification product was used. In order to ensure that appropriate pixel registration would not introduce error into the study, the MODIS land cover product was chosen over other land cover datasets. The Aqua/Terra combined MCD12Q1 has five land cover types data subsets from the International Geosphere Biosphere Program (IGBP), the University of Maryland, MODIS LAI/fPAR, MODIS Net Primary Production (NPP), and Plant Functional Type (PFT). These land cover types can be useful for specific applications and areas, and have different of classes and vegetation types. See table 2 for a listing of land cover classes with each classification scheme.

Table 2. MCD12Q1 Land Cover Classes

Class	IGBP (Type 1)	UMD (Type 2)	LAI/fPAR (Type 3)	NPP (Type 4)	PFT (Type 5)
0	Water	Water	Water	Water	Water
1	Evergreen Needleleaf forest	Evergreen Needleleaf forest	Grasses/Cereal crops	Evergreen Needleleaf vegetation	Evergreen Needleleaf trees
2	Evergreen Broadleaf forest	Evergreen Broadleaf forest	Shrubs	Evergreen Broadleaf vegetation	Evergreen Broadleaf trees
3	Deciduous Needleleaf forest	Deciduous Needleleaf forest	Broadleaf crops	Deciduous Needleleaf vegetation	Deciduous Needleleaf trees
4	Deciduous Broadleaf forest	Deciduous Broadleaf forest	Savanna	Deciduous Broadleaf vegetation	Deciduous Broadleaf trees
5	Mixed forest	Mixed forest	Evergreen Broadleaf forest	Annual Broadleaf vegetation	Shrub
6	Closed shrublands	Closed shrublands	Deciduous Broadleaf forest	Annual grass vegetation	Grass
7	Open shrublands	Open shrublands	Evergreen Needleleaf forest	Non-vegetated land	Cereal crops
8	Woody savannas	Woody savannas	Deciduous Needleleaf forest	Urban	Broad-leaf crops
9	Savannas	Savannas	Non-vegetated		Urban and built-up
10	Grasslands	Grasslands	Urban		Snow and ice
11	Permanent wetlands				Barren or sparse vegetation
12	Croplands	Croplands			
13	Urban and built-up	Urban and built-up			
14	Cropland/Natural vegetation mosaic				
15	Snow and ice				
16	Barren or sparsely vegetated	Barren or sparsely vegetated			
254	Unclassified	Unclassified	Unclassified	Unclassified	Unclassified
255	Fill Value	Fill Value	Fill Value	Fill Value	Fill Value

The scheme used in this project was the IGBP primary land cover classification from 2012. This product was chosen based on its temporal relevance and increased spatial resolution compared to other land cover datasets such as the Global Land Cover Characterization GLCC, which was a 1km global product created in 2000. In addition,

the increased number of classes from the IGBP over there four classification schemes in the MODIS product is more useful to understand the variations of NDVI within each land cover type in the varying topography of the landscape. The IGBP has 17 land cover classifications as shown below and in table 2. The IGBP dataset is used in this study to identify NDVI characteristics of each land cover type within the baseline, explained in the next sections.

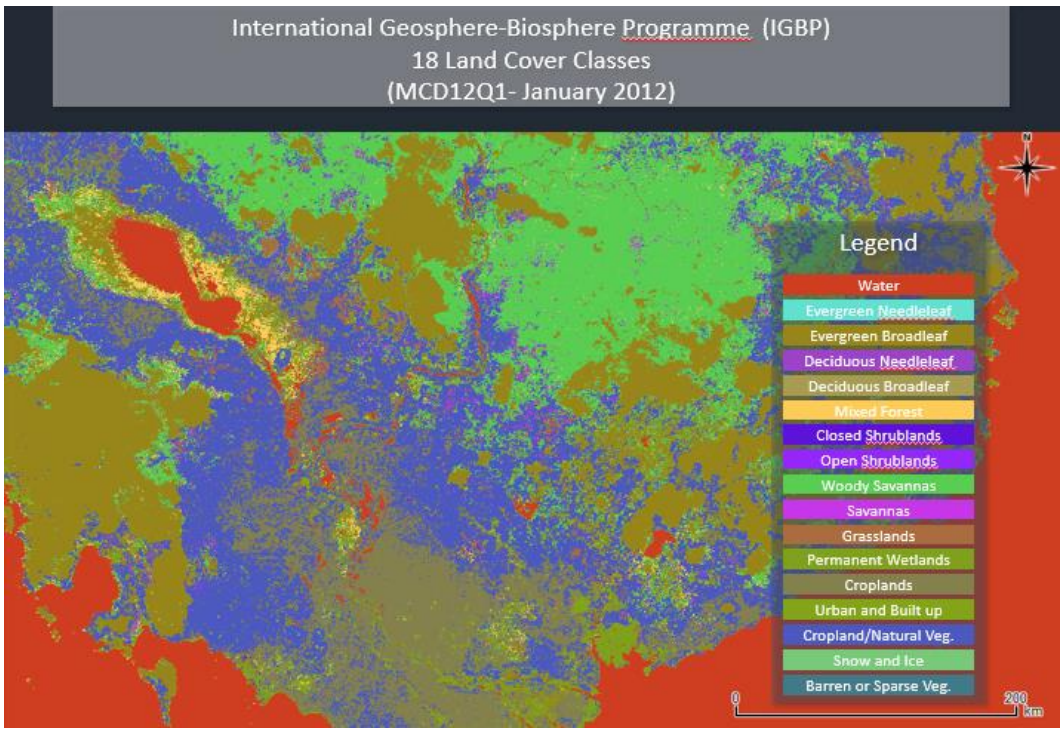

Figure 22 Map with land cover and 17-class legend

Ancillary datasets to support the understanding and limitations of data products are especially important to this study, as NDVI decrease can by associated with many variables, regardless of the season. For instance, fires can cause a drastic decline in

NDVI, and post fire areas experience declining NDVI for weeks following the fire event (Goetz, Fiske and Bunn 2006, Peckham, et al. 2008). Because fires and other factors other than flooding can contribute to decreasing NDVI, it is important to integrate many datasets to remove bias associated with the assumption that flooding is the cause of NDVI decrease. This will also support the NDVI decrease-flood assumption, as the size of the area affected from flooding during the flood season is much larger and more noticeable from space than fires in this region. As an example for how additional datasets can support the NDVI decrease from flooding assumption in the area, the addition of fire data from the Aqua and Terra MODIS daily 1-km fire product (MOD14A1) was added to the final classification scheme. Future work on the product visualization and classification should also incorporate more relevant datasets as they become available.

The IGBP classification scheme is used in this study to understand the relationship between NDVI of the baseline image and land cover at each NDVI location. This association will guide future research towards creating masks based on expected flooding of particular land cover classes as well as finding trends in NDVI before, during, and after the flood season. The association of the 2012 IGBP land cover dataset was completed in the R statistical programming language, where the mean and standard deviation values of the baseline NDVI were calculated for each land cover class as follows:

```
LC<-(as.matrix(raster("E:/Data/thesis/baselineimage/landcoverIGBP_2012_250m.tif")))
Baseline<-(as.matrix(raster("E:/Data/thesis/baselineimage/baseline/Finalmean.tif")))
STDDev<-(as.matrix(raster("E:/Data/thesis/baselineimage/baseline/sdev.tif")))
DateObservation<-(as.matrix(raster("E:/Data/thesis/dailyimages/composites/November.tif")))

BaseLC0<-mean(Baseline[LC==0])
BaseLC1<-mean(Baseline[LC==1])
BaseLC2<-mean(Baseline[LC==2])
BaseLC3<-mean(Baseline[LC==3])
BaseLC4<-mean(Baseline[LC==4])
BaseLC5<-mean(Baseline[LC==5])
BaseLC6<-mean(Baseline[LC==6])
BaseLC7<-mean(Baseline[LC==7])
BaseLC8<-mean(Baseline[LC==8])
BaseLC9<-mean(Baseline[LC==9])
BaseLC10<-mean(Baseline[LC==10])
BaseLC11<-mean(Baseline[LC==11])
BaseLC12<-mean(Baseline[LC==12])
BaseLC13<-mean(Baseline[LC==13])
BaseLC14<-mean(Baseline[LC==14])
BaseLC15<-mean(Baseline[LC==15])
BaseLC16<-mean(Baseline[LC==16])
```

Figure 23. Script to calculate the mean baseline NDVI at each land cover class

With the following result:

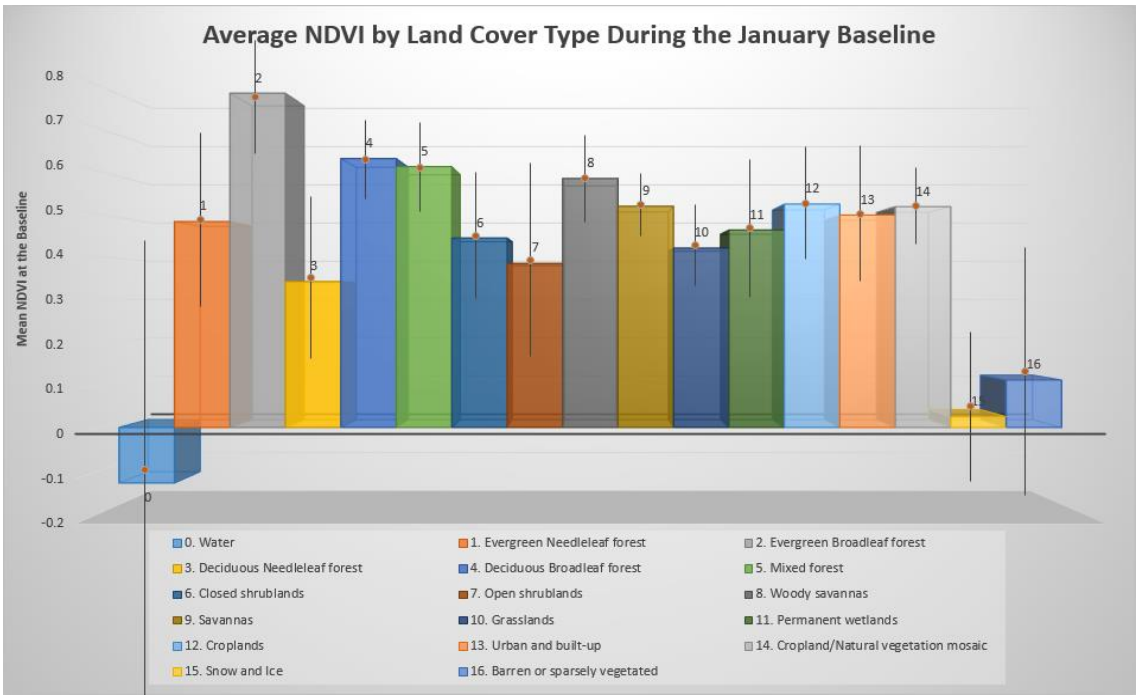

Figure 24. The mean and standard deviation values of Baseline NDVI at each land cover class

The means and standard deviations for each land cover show the expected values for each class. It is generally agreed that classes such as urban areas, water, snow/ice, and barren land will have very low NDVI values. One of the limitations of this chart is uncharacteristically high values for urban areas, which may be due to mixed pixels and the proximity of urban areas to healthy vegetative areas near water bodies. The mean NDVI for each land cover calculation was used again for each daily observation.

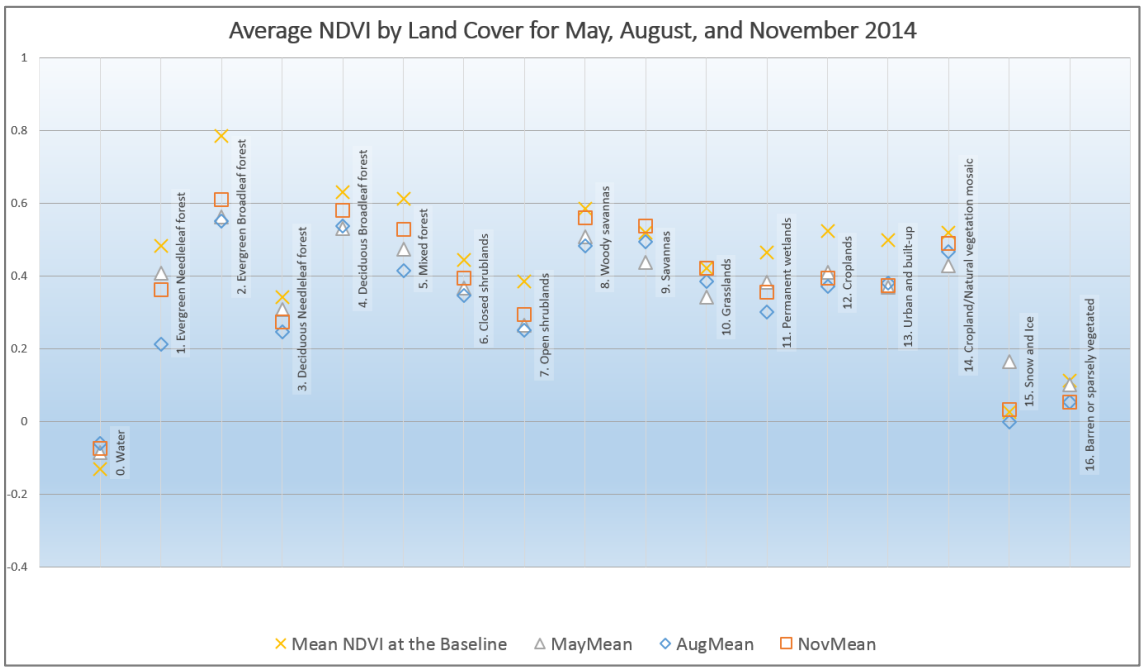

Figure 25. The NDVI for each daily observation for land cover

The NDVI for water bodies are characteristically low, the only land cover class with a consistently negative NDVI in this study, which supports the idea that water has a low NDVI value. Specifically, the means for all observations suggested that water has a

consistently negative NDVI value. More statistical tests are needed to understand the relevance of the change within each land cover class during the observations dates.

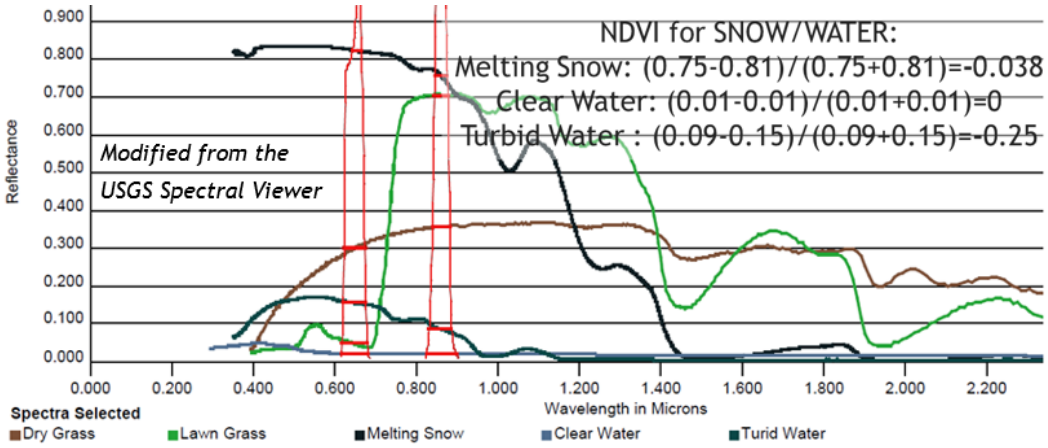

Figure 26. Spectral Signatures of Water and Vegetation

Negative values for NDVI in the water land cover classification suggest that water has a negative NDVI, which is further supported by the spectral signatures figure above, and therefore areas outside the permanent water land cover could be considered flooded when the NDVI decreases to negative values. Based on a review of different spectra that are common in the area and are visible at the 250-meter resolution, water is the only likely negative NDVI value, although at finer spatial resolution other features such as barren soils, concrete, or snow might have a negative NDVI value. Without comparing the daily data to the baseline date, only negative values are selected in each of the observations.

Figure 27. Negative NDVI from Composite Dates May 26-29, August 22-25, November 25-28

Validation of Classifications

The classification intervals attempted to describe the amount of the change from the baseline in terms of the percent difference, the difference in NDVI values, and the amount of standard deviations from the mean. In each case, the minimum value to report a difference is noted in table 3 below.

Table 3. Classification values

Scheme	Minimum Values to Detect Flood	Maximum Values
Percent Change (Doyle)	4% Decrease	100% Decrease
Equal Interval (Abbas)	20% Decrease	100% Decrease
Differencing (Song)	Difference -0.1 and Less	Difference -0.25 and Less
Standard Deviation (Sarp)	2 Standard Deviations Below the Mean	9 Standard Deviations Below the Mean

The classifications are compared with the negative NDVI map from figure 26, as one measure to validate the classifications against the areas of likely flooding. A limitation of this accuracy assessment and the following accuracy assessment of the proposed classification is the lack of ground truthing in the area. As the negative NDVI values are all assumed to be water based on the previous section, this serves as a useful first test to determining which classification is more closely related to flood water, and which intervals are more useful for matching with the negative NDVI flood region. Figure 28 below shows a chart of the accuracy results compared to the classification, as well as the maps of the negative NDVI overlap with three classifications with the highest Producer's and User's accuracy.

The accuracy assessment was completed in R and compared the entire pixel population of the classifications to the entire pixel population of the reference dataset. The accuracy assessment was conducted by converting the negative NDVI values and the classification values of interest into new binary matrices of 'flood=1' or 'not flood=0'. A new 'match' matrix is created where both matrices are added to create values ranging from 0-2, and 2=match. Producer's accuracy is defined as the ratio of matches or true

positives to the number of actual observations from the reference dataset; User's accuracy is defined at the ratio of true positives within the classification.

```
DateObservation<-(as.matrix(raster("E:/Data/thesis/dailyimages/composites/August.tif")))
#this is the actual NDVI for the specific date
Percent<-(as.matrix(raster("E:/Data/thesis/anomaly/Doyle_percent/DoyleAugNewBase.tif")))
# this is the classification using a percent change from the baseline
WaterMask<-(as.matrix(raster("E:/Data/thesis/baselinsimage/new_landwater.tif")))
#this is the permanent water mask where land is 1 and water is 0
OnesPercent100<-1*(Percent> -6000 & Percent< -100)
#Segment the values with decreases below -100 (Percent decreases lower than 6000 are generally noise from water reflectance)
OnesDate<-1*(DateObservation> -1.1 & DateObservation< 0)
#Segment the values with negative NDVI values (negative values are water based on earlier analysis)
OnesDate<-OnesDate*WaterMask
OnesPercent100<-OnesPercent100*WaterMask
#remove ocean and other permanent water
a<-(OnesDate+OnesPercent100)
#add the 1s from the two segmentations
b<-1*(a==2) # where the 1s overlap
ProducersAccuracy<-(sum(b))/(sum(OnesDate))
UsersAccuracy<-(sum(b))/(sum(OnesPercent100))
```

Figure 28. Accuracy Assessment R Script

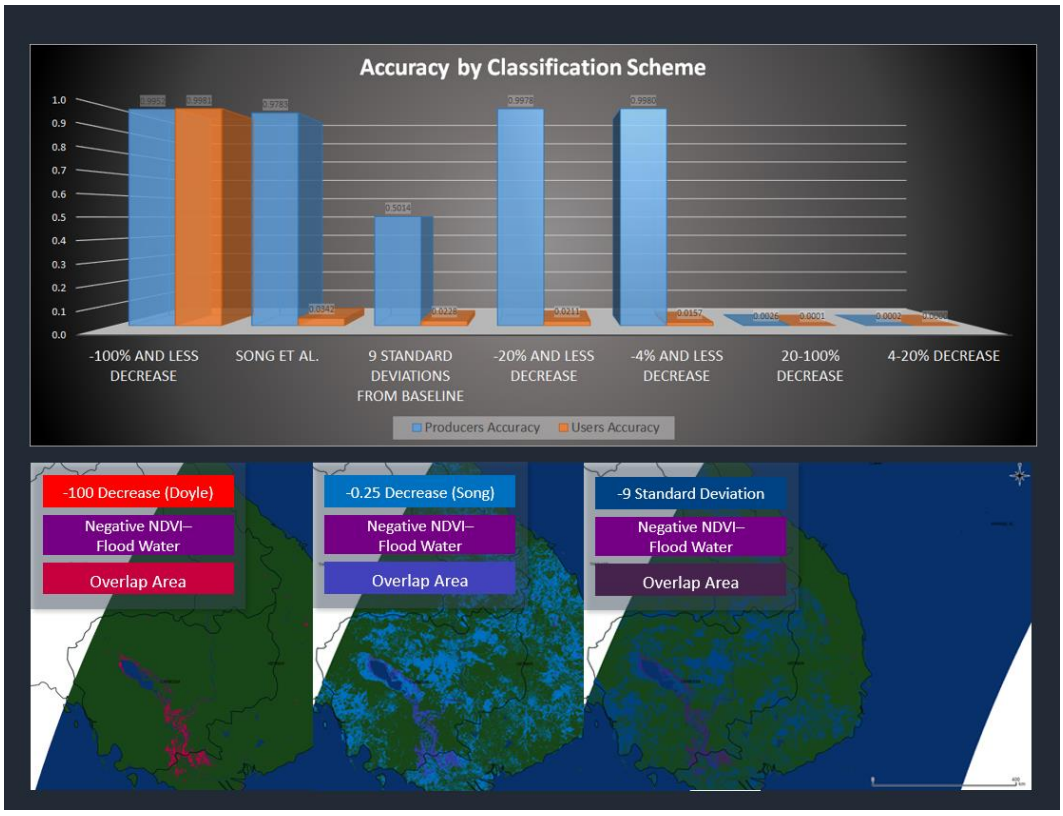

Figure 29. Accuracy by Classification Scheme

The accuracy from the 100% and more decrease levels are more closely associated with flooding based on the negative NDVI reference data. The 100% change is much more narrowly confined to the floodplain in contrast to the -0.25 decrease method from (Song, et al. 2004) and the standard deviation method from (Sarp 2011), where the flooded areas are accurately, but not precisely defined compared to the negative NDVI 'flood' areas. Further, the 4-100% decrease range matched less than 1% of the flooded areas, and therefore are not useful classes for this purpose and spatial resolution.

Final Proposed Classification

Because this ground truthing is not available, the classification validation is limited to the data sources available for that location, proximal to the time of acquisition to the dataset to be validated. The nature of the composite dataset poses a special problem for validation because of cloud cover in the area. The composite dataset was created by removing the clouds and backfilling the dataset with data from previous dates. This is a useful method for monitoring floods in near-real time, but poses difficulty when comparing it with imagery from a single date.

Based on the accuracy assessment from the previous section, it is clear that the 100% decrease interval is the best for classifying floods in the region, while the 4-100% is not useful for mapping visible flooding. This assessment suggests the creation of a new classification scheme with only two classes: 'wet' and 'flooded', where the 'wet' areas are defined from the 75% interval class as it is approaching the 100% interval, but does

not fully meet the criteria for visually flooded areas. Using the 75% interval is useful where mixed pixels or canopy cover can underestimate the amount of water on the ground, and provides an alert to areas that may become flooded. The 100% interval range can be classified as confidently flooded based on the assessment with the MODIS negative NDVI data. As values can far exceed the 100% interval into 200% and 300% decrease, future work may help to determine what larger decreases in NDVI mean for the relationship with flooding. At the same time, an analysis of the 4-50% classes should be assessed for evidence of flooding in subpixel areas or change due to natural variation, this might be done using the Open Water Likelihood method previously mentioned in the literature to determine what percent of the pixel is likely to have water.

The interval classification was created for all processed data with QGIS and ArcMap software, with the exception of the standard deviation classification. The new classification does not require any additional processing because it is the same data that was used in the Doyle and Abbas classification, but with fewer intervals. For integration into the Online Dashboard the data can be binned and reprocessed into two distinct categories for ease of viewing and downloading the product. Similarly, an earlier iteration of the DEVELOP product used the actual percent change values but were classified according to the six interval categories. Using the actual decrease values significantly slowed drawing time on the website, which was a major problem when panning and zooming in on features in the image, which lead the team to transform the values in the image to match the distinct interval categories. Additionally, further simplification of the

flood extent product will increase the drawing and loading time improve the use of the product on the website.

Figure 30. 75/100% Flood Product with imagery from ArcMap 'Imagery with labels' basemap. The Online Product will appear with a choice between labeled Google Earth Imagery, or Google Maps vector features

While this product is a departure from the original classifications suggested, the use of two classes allows the viewer to more easily interpret the differences between two colors of the same family rather than a spectrum of colors, or a color ramp with indistinguishable differences between intervals. In addition, the descriptive naming eliminates the need for the user to have any knowledge of the scientific process that served to create the data, simply answering the question of whether or not an area is flooded, as expected with a flood product.

Validation against MODIS and Landsat 8

The August 25 observation 100% decrease product was validated against the MODIS Negative NDVI again, as well as dark pixel values from MODIS surface reflectance band 2 infrared composite, and a Landsat 8 observation. Because of persistent cloud cover during this time, and 16-day revisit cycles of the Landsat 8 sensor, it was difficult to find an appropriate date to compare the classification for the August 25 observation. The closest date to the August 25 observation from Landsat 8 is September 9, 2014, which has been characterized as having 37.42% cloud cover in the scene. Because of the existing cloud cover in the reference dataset, the validation results were expected to be lower than if the full scene was clear. The ideal Landsat scene date for August 24 reports 60.94% cloud cover, where the clouds completely obscure flooding in the area.

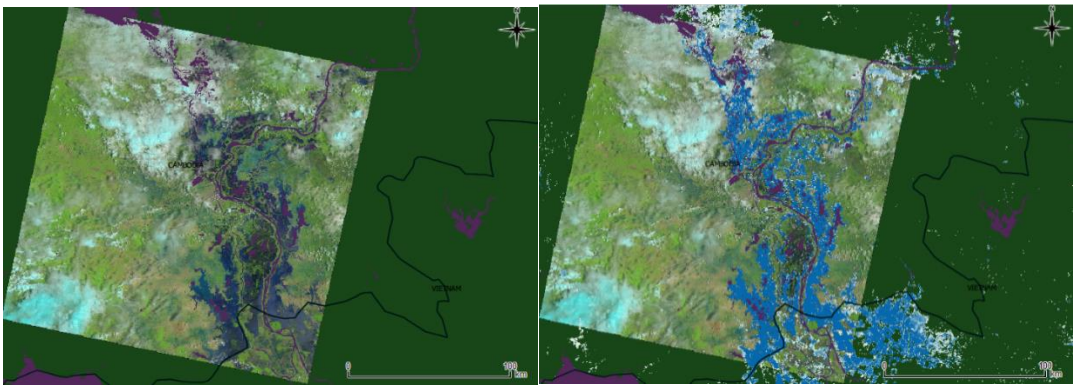

Figure 31. Landsat Scene with the Proposed Classification

The validation process for the MODIS Negative NDVI (composite), MODIS IR Surface Reflectance (composite), and Landsat 8 IR (not atmospherically corrected) was a similar process as explained when each of the classification intervals were compared to the Negative NDVI. The percent change image was read into R and converted into a matrix of 1s where the decrease was 100% or more, and 0s for everything else. The dark pixel threshold value for the MODIS IR Surface Reflectance was less than 1,000, and the dark pixel threshold value for Landsat 8 IR was less than 11,500. In both IR bands, zero values were ignored as background values. This method is effective for matching all of the pixels in the scene reducing bias in selecting how many pixels are counted and assessed, or selecting the sample region. With the exception of the Landsat 8 scene, which is a spatial subset of the overall study area, all classified pixels were compared with their counterparts in the reference datasets. The Landsat 8 scene however has a spatial bias as the Landsat pixels were down sampled to the MODIS 250 meter resolution for pixel comparison, and the extent—pixels with no data—were added to match the full extent of the MODIS tile.

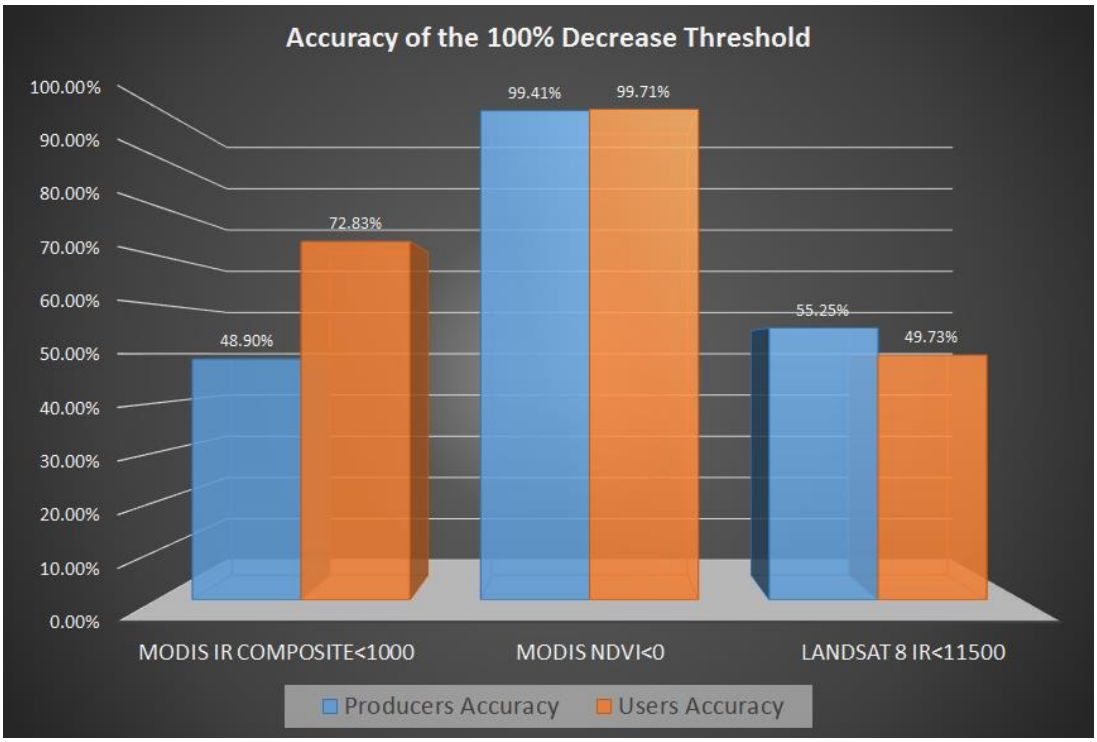

Figure 32. Accuracy Assessment Graph

Table 4. Error Matrix

Reference Data	Producers Accuracy	Users Accuracy
MODIS IR Composite<1000	48.90%	72.83%
MODIS NDVI<0	99.41%	99.71%
Landsat 8 IR<11500	55.25%	49.73%

		Accuracy Rating MODIS and Landsat Reference Data						#Classified Pixels
		MODIS IR		MODIS NDVI		Landsat 8 IR		
		Flood	Not	Flood	Not	Flood	Not	
NDVI	Flood	69826	26047	95591	282	47677	48196	95873
100%	Not	72954	22871173	568	22943559	38610	22905517	22944127
#Reference Pixels		142780	22897220	96159	22943841	86287	22953713	23040000

Because of the real-time nature of this dataset, very few opportunities exist to validate against other datasets. The Landsat 8 data is most commonly used for this purpose due to its relatively high resolution and frequent revisit times, however persistent cloud cover remains a problem for comparison. One solution for future validation attempts would mask out areas with clouds and only compare areas where the surface is exposed in both datasets. Future validation efforts will involve comparing the 100% decrease threshold with the Near Real-Time Global Flood Mapping Product (Nigro, et al. 2014).

DISCUSSION

Several components of this study required an understanding of the physical principles of land surface processes, as well as remote sensing and specialized data types in order to streamline an existing flood detection product to be used by a wider user base. To do this research, basic programming was necessary to compute the relationships between large images sets, to extract information about image relationships, and to transform reflectance data into meaningful, descriptive information.

Land Cover Information Integration with NDVI Decrease

The use of land cover in this study was pivotal in the creation of the new flood classification product based on NDVI percent decrease. Land cover can be used as a mask for flooded areas that are highly unlikely to flood due to their proximity to rivers or waterbodies that are prone to overflow. In addition, while floods might occur in land cover types such as deciduous broadleaf, forest density and canopy cover may obscure the area to be detected by the sensor. This is particularly important at the coarse spatial resolution where forests boundaries and gaps are indistinguishable.

This study used the IGBP land cover classification based on the amount of available classes to begin to have a clearer understanding of the expected NDVI, also known as a ‘greenness’ index. Future research on the use of land cover for flood mapping in this region might also integrate the Leaf Area Index, which is a measure of leaf density, to determine an appropriate threshold where the sensor would be able to detect floods in forests. Incorporating an index such as the leaf area index as well as ground

observations can help to determine the how mixed pixels can be categorized for flooding, as this principal study seeks to find very clearly defined flood boundaries at 250 meter resolution. NDVI decrease due to mixed pixels might be due to flooding underneath sparse canopy, while NDVI decrease in dense vegetation at a coarse spatial resolution is unlikely to indicate flooding, but an actual change in vegetation health. Focusing more on the sensor parameters, the Aqua and Terra satellites have opposite orbital paths, which can allow the sensors to see physical features from an opposing perspective.

Three land cover classes have been identified as having a mean NDVI value of below 0.2: Snow/Ice and Barren Land generally have low NDVI, but also have variability even during the dry season observations, although the results from the standard deviation calculation might be skewed by cloud contamination. In this study area, water is the only land cover class with a mean negative NDVI value, which indicate that negative values might be a characteristic for water overall. During the summer months, the snow and ice classification dropped just slightly for as a possible indicator for melt or increased surface water from rainfall.

Further study on these variations based on ground observations more very high resolution imagery are necessary to understand the differences between seasonal trends and changes in land cover and major events such as flooding in the region. Because the NDVI baseline consists of January only observations for peak greenness, NDVI values are expected to decline through the year, and it is important not to confuse small rates of change from seasonality with flood events. Preliminary steps in the future study would take the weekly mean of the land cover classes to track variation over time. Sudden,

persistent drops in NDVI for the land cover during the monsoon season, and a recovery at the beginning of the year might indicate the presence of flooding, which will appear spectrally different for each land cover type.

The use of negative NDVI to support the percent change classification might seem redundant. If negative NDVI explains the presence of water, then perhaps the percent change classification is not necessary. Particularly in this case, the 75% decrease class is outside of the scope of negative NDVI, signaling a large amount of change in the greenness of an area, while not fully asserting that the area is flooded. More broadly, the use of percent change lends itself to being able to capture change in mixed pixels, instead of an exact value. Many anomaly studies are used in cases where the physical phenomena are not visually apparent such as drought. Where the canopy cover is minimal in crop fields commonly found in the area, flooding is easily observable from space using surface reflectance bands, however areas that may flood in the near future are less noticeable and require additional processing as seen with the NDVI change method.

Furthermore, the area of interest consists primarily of cropland that is intentionally flooded as part of regular farming practice. A more thorough understanding of crop types and associated farming schedule will help to separate areas that are intentionally flooded from living spaces and towns in close proximity to farmlands.

The classification examples in this text depict information from the same three dates in a variety of different ways to demonstrate how visualization and categorization of a product can drastically change user perception of the product utility. All of the classification examples remained quantitative, explaining ‘how much’ but not ‘why’. No

color change or grouping could provide enough meaningful data for users to understand the same information in the same way. Because this product used NDVI as the only variable, it is particularly susceptible to error during dry seasons, when drought is common, which will then be assumed flooded in a flood related product.

The percent change product is particularly useful in this case, as the change calculation brings uniformity to the whole study region. The NDVI decrease value of 100 and more very closely match water categorized from surface reflectance and negative NDVI values without comparison to a baseline.

Flood Mapping Literature for the Visualization of the Percent Change Product

Many of the flood maps reviewed focus less on the input data and more on the purpose of the product to explain where floods exist. In doing so, flood maps often have binary classifications of flooded/not flooded areas, or incorporate a second component entirely such as flood depth (Lant 2013), or previous flood extent (Brakenridge, Anderson and Caquard 2004).

Users might be confused with the variable interval boundary lines and what that means for the status of water in a six-interval classification product when they are used to using only one class. Further, while the subtle changes in blue shading are also undesirable, the use of two separate color ramps—dark blue to green, then yellow to red might also pose a challenge to users. Conversations with two domain experts in the field of remote sensing and spectral indices revealed that because of the amount of features classified in the study area, it was difficult to distinguish background from mapped features, and which areas were actually flooded. However, because the original

classification used very distinct color intervals, classes were much easier to distinct, and patterns could be found in the image. One expert noted that there was no distinct pattern in the scene; flooding should occur very close to the water bodies, and that none of the classifications were usable because they all mapped features in all regions of the study area. Because the proposed product eliminates many decrease classes, formal testing on user perception of color use is less necessary, as only two distinct colors will be used to define flooded areas and areas that might soon become flooded. When asked about the final classification, both reviewers noted that while the descriptive classification based on two of the percent decrease intervals was visually more appealing. It was also noted that the small regions of still classified pixels very far from the Mekong River and Tonle Sap Lake were 'noise' and it was suggested that a filter over the scene be used to remove very small classified areas.

Flood maps generally have a narrowly defined purpose which dictate their use and input data such as current information emergency response or historical data for flood risk mapping or land use planning. Flood depths (Lant 2013) provide a useful dynamic to flood maps to give the user specific information about the inundation level and the type of risks that exist in that area. However, mapping flood depth can be difficult when the elevation model in use is outdated or has a much more coarse spatial resolution than the extend product. Future efforts will involve the integration of flood depth information for the 75%-'wet-not flooded' and 100%-'flooded' classifications to calibrate the product to reduce over or under detecting flooded area in deep or shallow terrain.

Understanding Baseline NDVI values

The difference from the baseline method described in (Song, et al. 2004) was expected to yield a product that closely matched flooded areas, based on the amount if decline experienced from the baseline date. However, as the observations dates showed a uniform decline throughout the scene, the differencing method was not precise enough to explain flooding as threshold difference from the mean values. This finding was also consistent with the standard deviation, where there is a uniform decline in the baseline, but the intervals defined did not clearly explain any flooding in the region. The percent change method might have been an exception in this case due to the many intervals, which explained the amount of change at each level. The baseline NDVI values ranged from -0.3 to 1 during peak greenness; the recalculation of the baseline mean values was not beneficial without the additional grouping by land cover classes. Flooding due to deviations from the base values cannot be assumed without additional comparison with land cover classes and reference datasets. While the differencing and standard deviation methods failed to accuracy classify flooding, only one class of the percent change intervals was able to classify flooded areas accurately and precisely.

Creating the new descriptive classification will help users to incorporate the new mapping product with other datasets such as historical flood maps, precipitation monitoring, hydraulic models and other information of interest.

CONCLUSION

To monitor flooding in the lower Mekong River Basin, a near-real time NDVI percent decrease based Flood Extent Product was developed to be hosted on an online Flood Dashboard by the NASA DEVELOP team. The real-time product was designed to update twice per day with 250-meter resolution from MODIS on the Aqua and Terra satellites with classification intervals of 4, 15, 30, 50, 75, and 100% change from a mean baseline value from years of January observations. Low NDVI values are commonly associated with unhealthy vegetation, barren land, snow and water, which makes NDVI decrease an alternative to measuring flooding directly. However, using NDVI presents an additional problem for users who have little or no understand of the implications of NDVI or associated change from a baseline. Further, the interval classifications presented in the original product explains all features in the image, and not an exact event. To increase the usage and understand of this product, the classification intervals were compared with other commonly used classification schemes to monitor flooding.

While NDVI decrease can be associated with many factors, studies involving NDVI change generally focus on narrower amounts of change. Small amounts such as 4% change for defoliation due to moth infestation (Spruce, et al. 2011) and 30% maximum observed decrease from drought (Murad and Saiful Islam, Drought Assessment using remote sensing and GIS in North-West region of Bangladesh 2011), -0.25 difference for drought mapping (Song, et al. 2004) are common, but not universally applicable. This study is unique in focusing on higher rates of change as seasonal minor variations are expected.

This study concluded that by land cover type, water consistently has a negative NDVI unlike any other land cover class, and higher rates of NDVI change can be associated with the presence of water in areas that regularly have healthy vegetation, particularly during the flood season. This study also provides opportunities for future studies in flood mapping in the region using additional land cover datasets such as LAI, and using elevation models to derive flood depth.

REFERENCES

Abbas, Sawaid, Janet E. Nichol, Faisal M. Qamaer, and Jianchu Xu. 2014. "Characterization of Drought Development through Remote Sensing: A Case Study in Central Yunnan, China." *Remote Sensing* 4998-5018.

Ali, Anwar, Dewan A. Quadir, and Oscar K. Huh. 1989. "Study of river flood hydrology in Bangladesh with AVHRR data." *International Journal of Remote Sensing* 1873-1891.

Anderson, Martha C., John M. Norman, John R. Mecikalski, Jason A. Otkin, and William P. Kustas. 2007. "A climatological study of evapotranspiration and moisture stress across the continental United States based on thermal remote sensing: 1. Model formulation." *Journal of Geophysical Research: Atmospheres* 1-17.

Boshetti, Mirco, Francesco Nutini, Giancinto Manfron, Alessandro Pietro Brivo, and Andrew Nelson. 2014. "Comparative Analysis of Normalised Difference Spectral Indices Derived from MODIS for Detecting Surface Water in Flooded Rice Cropping Systems." *PLOS*, February.

Brakenridge, Robert, and Elaine Anderson. 2006. "MODIS-Based Flood Dectection, Mapping and Measurement: The Potential for Operational Hydrological Applications." In *Transboundary Floods: Reducing Risks Through Flood Management*, by Jiri Marsalek, Gheorghe Stancalie and Gabor Balint, 1-12. Amsterdam: IOS Press, | Springer.

Brakenridge, Robert, Elaine Anderson, and Sebastien Caquard. 2004. *Rapid Response Inundation Map: DFO Event # 2004-144 Vietnam and Cambodia Lower Mekong.* September. http://www.dartmouth.edu/~floods/images/2004144Mekong.jpg.

Cai, Gouyin, Mingyi Du, and Yang Liu. 2010. "Regional Drought Monitoring and Analyzing Using MODIS Data- A Case Study in Yunnan Provice." In *Computer and Computing Technologies in Agriculture IV*, 243-251. Nanchang: China.

Carlson, J, and J Burgan. 2003. "Review of Users' Needs in Operational Fire Danger Estimation: The Oklahoma Example." *International Journal of Remote Sensing* 1601-1620.

Carroll, Mark, J Townshend, C DiMiceli, P Noojipady, and R Sohlberg. 2009. "A New Global Raster Water Mask at 250 Meter Resolution." *International Journal of Digital Earth* 291-308.

CEOS WGDisasters. 2015. *Flood Pilot | Committee on Earth Observing Satellites Working Group on Disasters.* http://ceos.org/ourwork/workinggroups/disasters/floods/.

Chen, Yun, Chang Huang, Catherine Ticehurst, Linda Merrin, and Peter Thew. 2013. "An Evaluation of MODIS Daily and 8-day Composite Products for Floodplain and Wetland Inundation Mapping." *Wetlands* 823-835.

Colwell, John E. 1974. "Vegetation Canopy Reflectance." *Remote Sensing of Environment* 175-183.

Doyle, Colin, Amanda Rumsey, Jessica Fayne, and Alexander Nelson. 2014. *NASA DEVELOP Team Report.* Hampton, VA: NASA DEVELOP.

e-GEOS. 2011. *City of Water: October 2011 Flood Boundaries (Phnom Penh, Cambodia).* October 14. https://cityofwater.files.wordpress.com/2012/05/281middle-safer_gers108_eg01_flood_cambodia_disasterextentmap.jpg.

Frazier, Paul Shane, and Kenneth John Page. 2000. "Water Body Detection and Delineation with Landsat TM Data." *Photogrammetric Engineering and Remote Sensing* 1461-1467.

Gallant, John C., and Trevor I. Dowling. 2003. "A multiresolution index of valley bottom flatness for mapping depositional areas." *Water Resources Research* 4- 1-14.

Gao, Bo-cai. 1996. "NDWI- A normalized difference water index for remote sensing of vegetation liquid water from space." *Remote Sensing of Environment* 257-266.

Goetz, Scott J., Gregory J. Fiske, and Andew G. Bunn. 2006. "Using satellite time-series data sets to analyze fire disturbance and forest recovery across Canada." *Remote Sensing of Environment* 352-365.

Gopinath, Girish, G. K. Ambili, Shery Joseph Gregory, and C. K. Anusha. 2014. "Drought Risk Mapping of South-Western State in the Indian Peninsula--A web based application." *Journal of Environmental Management* 1-7.

Guerschman, Juan P, Garth Warren, Guy Byrne, Leo Lymburner, Norman Mueller, and Albert Van Dijk. 2011. *MODIS-based standing water detection for flood and large reservoir mapping_ algorithm development and applications for the Australian continent.* Report, Commonwealth Scientific and Industrial Research Organization.

Holben, Brent N. 2007. "Characteristics of maximum-value composite images from temporal AVHRR data." *International Journal of Remote Sensing* 1417-1434.

Jönsson, A M, L Eklundh, M Hellström, L Bärring, and P Jönsson. 2010. "Annual changes in MODIS vegetation indices of Swedish coniferous forests in relation to snow dynamics and tree phenology." *Remote Sensing Environment* 2719-2730.

Lant, Jeremiah G. 2013. *Flood-Inundation Maps for a 6.5-Mile Reach of the Kentucky River at Frankfort, Kentucky.* Pamphlet to accompany Scientific Investigations Map 3278, USGS.

Laskey, Katherine Blackmond, Edward J Wright, and Paulo DaCosta. 2010. "Envisioning Uncertainty in Geopspatial Infromation." *International Journal of Approximate Reasoning* 209-223.

McFeeters, Stuart K. 1996. "The Use of the Normalized Difference Water Index (NDWI) in the delineation of open water features." *International Journal of Remote Sensing* 1425-1432.

Murad, Hasan, and A.K.M. Saiful Islam. 2011. "Drough Assessment using remote sensing and GIS in North-West region of Bangladesh." *Proceedings of the 3rd International Conference on Water & Flood Management.* 797-804.

—. 2011. "Drought Assessment using remote sensing and GIS in North-West region of Bangladesh." *Proceedings of the 3rd International Conference on Water & Flood Management.* 797-804.

Myneni, Ranga B., Forrest G. Hall, Piers J. Sellers, and Alexander L. Marshak. 1995. "The Interpretation of Spectral Vegetation Indexes." *IEEE Transactions on Geoscience and Remote Sensing* 481-486.

Nash, Maliha S., David F. Bradford, James D. Wickham, and Timothy G. Wade. 2014. "Detecting change in landscape greenness over large areas: An example for New Mexico, USA." *Remote Sensing of Enviroment* (Remote S) 152-162.

National Snow and Ice Data Center;. 2015. *NASA Distributed Active Archive Center (DAAC) at NSIDC: MODIS Data.* http://nsidc.org/data/modis/terra_aqua_differences/.

Nigro, Joseph, Daniel Slayback, Frederick Policelli, and Robert Brakenridge. 2014. "NASA/DFO MODIS Near Real-Time (NRT) Global Flood Mapping Product Evaluation of Flood and Permanent Water Detection." Evaluation, Greenbelt, MD.

NOAA SIS. 2013. *NOAA Satellite Information System: Advanced Very High Resolution Radiometer- AVHRR.* November 26. http://noaasis.noaa.gov/NOAASIS/ml/avhrr.html.

Peckham, Scott D., Douglas E. Ahl, Shawn P. Serbin, and Stith T. Gower. 2008. "Fire-induced changes in green-up and leaf maturity of the Canadian boreal forest." *Remote Sensing of Environment* 3594-3603.

Pettorelli, Nathalie, Jon Olav Vik, Atle Mysterud, Jean-Michel Gaillard, Compton J. Tucker, and Nils Chr. Stenseth. 2009. "Using the satellite-derived NDVI to assess ecological responses to environmental change." *Trends in Ecology and Evolution* 503-510.

Quayle, Brad, Ken Brewer, and Kelly Williams. 2005. "Monitoring Post-Fire Vegetation Recovery Of Wildland Fire Areas In The Western United States Using Modis Data." *Pecora 16 "Global Priorities in Land Remote Sensing"* . Sioux Falls: American Society of Photogrammetry and Remote Sensing. 1-10.

Ramsey III, Elijah, Dirk Werle, Yukihiro Suzuoki, Amina Rangoonwala, and Zhong Lu. 2012. "Limitations and Potential of Satellite Imagery to Monitor Environmental Response to Coastal Flooding." *Journal of Coastal Research* 457-476.

Rasid, Harun, and M.A.H. Pramanik. 1990. "Visual Interpretation of Satellite Imagery for Monitoring Floods in Bangladesh." *Environmental Mangement* 815-821.

Roth, Robert, David Hart, Rashauna Mead, and Chloe Quinn. 2014. "Design Before You Code: Using Wireframes in Support of Interactive & Web-Based Mapping." *AutoCarto.*

Rouse Jr., John W., R H Haas, J A Schell, and D W Deering. 1973. *Monitoring the Vernal Advancement and Retrogradation (Greenwave Effect) of Natural Vegetation.* Type II Report, Greenbelt, Maryland: Goddard Space Flight Center, 1-93.

Sarp, Gulcan. 2011. "Determination of Vegetation Change Using Thematic Mapper Imagery in Afşin-Elbistan Lignite Basin; SE Turkey." *Procedia Technology* 407-411.

Song, X, G Saito, M Kodama, and H Sawada. 2004. "Early detection system of drought in East Asia using NDVI from NOAA/AVHRR data." *International Journal of Remote Sensing* 25: 3105-3111.

Spruce, Joseph P., Steven Sader, Robert Ryan, James Smoot, Philip Kuper, Kenton Ross, Donald Prados, et al. 2011. "Assessment of MODIS NDVI time series data products for detecting forest defoliation by gypsy moth outbreaks." *Remote Sensing of Environment* 427-437.

Swets, D.L., B.C. Reed, J.D. Rowland, and S.E. Marko. 1999. "A weighted least-squares approach to temporal NDVI smoothing." *ASPRS Annual Conference: From Image to Information, Portland, Oregon May 17-21.* Bethesda, MD: American Society of Photogrammetry and Remote Sensing.

Töyrä, Jessika, Alain Pietroniro, Lawrence W. Martz, and Terry D. Prowse. 2002. "A multi-sensor approach to wetland flood monitoring." *Hydrological Processes* 1569-1581.

Tucker, Compton J. 1979. "Red and Photographic Infrared Linear Combinations for Monitoring Vegetation." *Remote Sensing of the Environment* 127-150.

U.S. Department of the Interior; U.S. Geological Survey;. 2014. *Vegetation Indices Monthly L3 Global 1km.* April 14. Accessed March 26, 2015. https://lpdaac.usgs.gov/products/modis_products_table/myd13a3.

U.S. Geological Survey; U.S. Department of the Interior;. 2014. *Land Processes Distributed Active Archive Center.* April 14. https://lpdaac.usgs.gov/products/modis_products_table/mod09q1.

U.S.Geological Survey. 2015. *Landsat Missions Timeline.* http://landsat.usgs.gov/about_mission_history.php.

van Dijk, Albert, Susan L. Callis, Clarence M. Sakamoto, and Wayne L. Decker. 1987. "Smoothing Vegetation Index Profiles: An Alternative Method for Reducing Radiometric Disturbance in NOAA/AVHRR Data." *Photogrammetric Engineering and Remote Sensing* 1059-1067.

Wang, Lingli, and John J. Qu. 2007. "NMDI: A normalized multi-band drought index for monitoring soil and vegetation moisture with satellite remote sensing." *Geophysical Research Letters* 1-5.

Xu, Hanqiu. 2006. "Modification of normalised difference water index (NDWI) to enhance open water features in remotely sensed imagery." *International Journal of Remote Sensing* 3025-3033.

Zhang, Xiaoyang, Mark A. Friedl, Crystal B. Schaaf, Alan H. Stahler, John C.F. Hodges, Feng Gao, Bradley C. Reed, and Alfredo Huete. 2003. "Monitoring vegetation phenology using MODIS." *Remote Sensing of Environment* 471-475.

BIOGRAPHY

Jessica V. Fayne graduated from Westfield High School, Chantilly, Virginia, in 2007. She received her Bachelor of Arts from Hampton University in 2010. She subsequently earned a graduate certificate in Cross Cultural Communications from American University in 2011. She was employed as an optician and office assistant in Fairfax County between 2010 and 2013, before entering the Master of Sciences program at George Mason University in August 2013.